Imperial College London

Monday, 22nd September 2014

Magnetic Monopoles in Pure Compact Lattice Quantum Electrodynamics

Nicholas William Prouse

Supervised by Professor Arttu Rajantie

Theoretical Physics Group
Department of Physics
Blackett Laboratory

Acknowledgements

"If my soul could get away from this so-called prison, be granted all the list of attributes generally bestowed on spirits, my first ramble on spirit wings would not be among the volcanoes of the moon. Nor should I follow the sunbeams to their sources in the sun. I should hover about the beauty of our own good star. I should not go moping among the tombs, nor around the artificial desolation of men. I should study Nature's laws in all their crossings and unions; I should follow magnetic streams to their source and follow the shores of our magnetic oceans. I should go among the rays of the aurora, and follow them to their beginnings, and study their dealings and communions with other powers and expressions of matter. And I should go to the very center of our globe and read the whole splendid page from the beginning."

From the diary of John Muir, 18th January 1870

Contents

1 Introduction

Since the earliest investigations into magnetism, it has been observed that magnets are formed of two poles and any attempt to separate the poles of a magnet results in two magnets, each still possessing both poles. The statement that an isolated pole of a magnet - a magnetic charge, or "monopole" - cannot exist without the opposite pole, meaning that magnetic field lines cannot begin or end at a source or sink, has never been seen to be violated.

However, the theoretical concept of a monopole was considered even before Maxwell's unification of electricity and magnetism. Electric charges do exist, with positive and negative charges providing the sources and sinks of electric field lines. This idea could be carried across to magnetic fields; in Maxwell's formulation of classical electromagnetism, there is nothing preventing the addition of magnetic charges. Doing so introduces the additional symmetry to the theory known as electric-magnetic duality, which - at least aesthetically - makes the unification of these two forces appear more natural.

In quantum theory, the situation is more complicated as the addition of monopoles seems to make the theory inconsistent due to quantum interference effects involving the vector potential. However, Dirac showed that there is no inconsistency so long as the monopole is restricted to having an integer multiple of a fundamental unit of magnetic charge that is proportional to the reciprocal of the electric charge. This not only implies that monopoles can be included without any need to alter the underlying theory, but also provides an explanation for the observed quantisation of electric charge. As noted by Dirac, "under these circumstances one would be surprised if Nature had made no use of it". In quantum electrodynamics (QED) though the mass of these Dirac monopoles is found to be infinite; even with the techniques of renormalisation their mass can still not be made finite. Once again, it seems that there is an obstacle to their existence even in theory.

However, QED is now known not to be the fundamental theory, but it emerges after symmetry breaking from the electroweak theory, which unifies electromagnetism and the weak nuclear force. Grand Unified Theories (GUTs) attempt to take the idea of unifying forces further, by combining all the forces of the Standard Model of particle physics into a single unified theory. 't Hooft and Polyakov found that such theories not only allow the existence of magnetic monopoles, but actually predict them. "Theories of everything", which include gravity in addition to the other forces, also

have this property. The mass of 't Hooft-Polyakov monopoles, unlike Dirac monopoles in QED, is finite, set by the energy scale of the symmetry breaking.

Despite having never been observed, the theoretical motivations for magnetic monopoles given above have prompted ongoing experimental searches for monopoles in a number of areas. As such it is important to understand their theoretical properties. One difficulty that arises is that the perturbative methods commonly used in performing calculations in quantum field theory are not appropriate in this case. Lattice gauge theories, on the other hand, provide a non-perturbative framework for studying gauge theories, formulating them on a discrete spacetime lattice. Furthermore, monopoles are found to exist on the lattice making it an obvious choice in which to study the monopole's properties.

Lattice gauge theories have been most widely used in studying the SU(3) theory of the strong nuclear force, Quantum Chromodynamics (QCD), another area where, at low energies, standard perturbation techniques are not appropriate. The understanding of confinement in QCD has been a major success of lattice field theory and monopoles have played a central role in this. Here, the lattice gauge theory known as compact U(1) will be studied, with the addition of a term in the action which is intended to reduce the suppression of monopoles and decrease their mass. In the continuum limit the compact U(1) gauge theory becomes the standard pure gauge form of QED - that is with only the gauge particle, the photon, and without fermions. By studying the properties of magnetic monopoles in this simple system, it may be possible to gain insights that also apply to physical monopoles that could exist in the more complex systems describing the real world.

2 Magnetic Monopoles

2.1 Magnetic Monopoles in Classical Electromagnetism

Maxwell's equations for classical electromagnetism can be written in the form[1]

$$
\begin{aligned}
\boldsymbol{\nabla} \cdot \mathbf{E} &= \rho_{\mathrm{E}} & -\boldsymbol{\nabla} \times \mathbf{E} &= \frac{\partial \mathbf{B}}{\partial t} \\
\boldsymbol{\nabla} \cdot \mathbf{B} &= 0 & \boldsymbol{\nabla} \times \mathbf{B} &= \frac{\partial \mathbf{E}}{\partial, t} + \mathbf{j}_{\mathrm{E}}
\end{aligned}
\tag{2.1}
$$

where $\mathbf{E}$ and $\mathbf{B}$ are the electric and magnetic fields respectively, ρ_{E} is the electric charge density and $\mathbf{j}_{\mathrm{E}}$ is the electric current density. In the absence of any electric charges, $\rho_{\mathrm{E}} = 0$, $\mathbf{j}_{\mathrm{E}} = 0$, the equations exhibit the symmetry known as electric-magnetic duality, characterised by the replacements

$$
\begin{aligned}
\mathbf{E} &\to \mathbf{B} \\
\mathbf{B} &\to -\mathbf{E},
\end{aligned}
\tag{2.2}
$$

which leave the equations invariant. However, the existence of electric charges breaks this symmetry, unless we also introduce magnetic charges known as monopoles. With the magnetic charge density $\rho_{\mathbf{M}}$ and magnetic current density $\mathbf{j}_{\mathbf{M}}$, Maxwell's equations become

$$
\begin{aligned}
\boldsymbol{\nabla} \cdot \mathbf{E} &= \rho_{\mathrm{E}} & -\boldsymbol{\nabla} \times \mathbf{E} &= \frac{\partial \mathbf{B}}{\partial t} + \mathbf{j}_{\mathrm{M}} \\
\boldsymbol{\nabla} \cdot \mathbf{B} &= \rho_{\mathrm{M}} & \boldsymbol{\nabla} \times \mathbf{B} &= \frac{\partial \mathbf{E}}{\partial t} + \mathbf{j}_{\mathrm{E}},
\end{aligned}
\tag{2.3}
$$

where the electric-magnetic duality is restored. The equations are now invariant under the substitutions

$$
\begin{aligned}
\mathbf{E} &\to \mathbf{B} & \rho_{\mathrm{E}} &\to \rho_{\mathrm{M}} & \mathbf{j}_{\mathrm{E}} &\to \mathbf{j}_{\mathrm{M}} \\
\mathbf{B} &\to -\mathbf{E} & \rho_{\mathrm{M}} &\to -\rho_{\mathrm{E}} & \mathbf{j}_{\mathrm{M}} &\to -\mathbf{j}_{\mathrm{E}}.
\end{aligned}
\tag{2.4}
$$

---

[1]Natural units, where quantities are given in units of the speed of light c, Planck's constant $\hbar$, the permittivity of free space ϵ_0, and the permeability of free space μ_0, i.e. $c = \hbar = \epsilon_0 = \mu_0 = 1$, have been used here and will be used throughout this report.

By combining the electric and magnetic fields into a single complex field, $\mathbf{E} + i\mathbf{B}$, the symmetry can be seen to correspond to a rotation in the complex plane. Maxwell's equations are then

$$\boldsymbol{\nabla} \cdot (\mathbf{E} + i\mathbf{B}) = \rho_{\mathrm{E}} + i\rho_{\mathrm{M}}$$
$$\boldsymbol{\nabla} \times (\mathbf{E} + i\mathbf{B}) = i\frac{\partial}{\partial t}(\mathbf{E} + i\mathbf{B}) + i(\mathbf{j}_{\mathrm{E}} + i\mathbf{j}_{\mathrm{M}})$$
(2.5)

which are now invariant under any complex rotation

$$\mathbf{E} + i\mathbf{B} \to e^{i\theta}(\mathbf{E} + i\mathbf{B})$$
$$\rho_{\mathrm{E}} + i\rho_{\mathrm{M}} \to e^{i\theta}(\rho_{\mathrm{E}} + i\rho_{\mathrm{M}})$$
$$\mathbf{j}_{\mathrm{E}} + i\mathbf{j}_{\mathrm{M}} \to e^{i\theta}(\mathbf{j}_{\mathrm{E}} + i\mathbf{j}_{\mathrm{M}}).$$
(2.6)

This all suggests that magnetic monopoles fit into classical electromagnetism in a very elegant way, allowing the theory to exhibit the additional symmetry of electric-magnetic duality. It is worth noting however that when describing the electric and magnetic fields in terms of the scalar potential ϕ and vector potential $\mathbf{A}$,

$$\mathbf{E} = -\frac{\partial \mathbf{A}}{\partial t} - \boldsymbol{\nabla}\phi$$
$$\mathbf{B} = \boldsymbol{\nabla} \times \mathbf{A},$$
(2.7)

it appears no longer possible for magnetic monopoles to exist, since

$$\rho_{\mathrm{M}} = \boldsymbol{\nabla} \cdot \mathbf{B} = \boldsymbol{\nabla} \cdot (\boldsymbol{\nabla} \times \mathbf{A}) = 0.$$
(2.8)

Nonetheless, this is not an argument for the non-existence of monopoles in classical electromagnetism. This is because this vector potential is not a physical object; the scalar and vector potentials are only defined up to a gauge transformation. Since the theory can be formulated entirely without these potentials, there is no theoretical obstacle to including magnetic charges. The vector potential does, however, form a fundamental part of the formulation of electromagnetism in quantum theory. In the next section it will be seen that this still does not preclude their existence; on the contrary, a large class of quantum field theories in which electromagnetism is embedded are found to inevitably contain monopole solutions.

2.2   Magnetic Monopoles in Quantum Field Theory

2.2.1   Dirac Monopoles

Despite the apparent implication of Equation (2.8), it is in fact possible to have a vector potential that describes a monopole at the expense of the vector potential being singular. The solution by Dirac [1] can be thought of as the magnetic field produced at the end of an infinitesimally thin solenoid that extends infinitely far in one dimension, known as a Dirac string. Since the magnetic field would be confined to within the solenoid except at the end where the magnetic field spreads out in all directions. The vector potential, in polar coordinates with the end of the Dirac string at the origin, is given by

$$\mathbf{A}(\mathbf{r}) = \frac{g\,\mathbf{r} \times \mathbf{n}}{4\pi r(r - \mathbf{r} \cdot \hat{\mathbf{n}})},$$
(2.9)

where $r = |\mathbf{r}|$, $\hat{\mathbf{n}}$ is a unit vector pointing out of the end of the solenoid, and g is the magnetic flux through the solenoid. This potential becomes singular at $\mathbf{r} = 0$, where the direction in undefined, but is otherwise smooth. The magnetic field described by such a potential exactly matches that produced by a monopole of charge g

$$\mathbf{B}(\mathbf{r}) = \frac{g\,\mathbf{r}}{4\pi r^3}.$$
(2.10)

In classical electromagnetism the solenoid itself is entirely unobservable and so the string can be thought of as being unphysical, leaving only an observable monopole. In quantum theory, however, charged particles can be affected by the vector potential (even in regions where the magnetic field is zero) due to the Aharonov-Bohm effect [2], by changing the complex phase of the particle's wavefunction. In the case of a Dirac solenoid, the complex phase φ of a particle of charge e moving along a closed loop will change by the amount

$$\Delta\varphi = e \oint \mathbf{A} \cdot d\mathbf{r} = e\Phi.$$
(2.11)

where Φ is the magnetic flux through the loop. This change in the complex phase is observable through interference effects unless $e\Phi$ is equal to an integer multiple of 2π. It would therefore be possible to have monopoles in quantum theory without an observable Dirac string (and hence the string could be considered to be unphysical with the monopole being the physical object), so long

as the electric and magnetic charges are quantised such that

$$\frac{eg}{2\pi} \in \mathbb{Z}. \tag{2.12}$$

This suggests that the existence of monopoles would explain the observed effect of charge quanti-sation, providing another - more concrete - theoretical indication for their existence, on top of the argument for preserving electric-magnetic duality.

The above discussion suggests that monopoles are allowed, and even expected, to exist in the quantum field theory of electromagnetism, quantum electrodynamics. However, there is an additional problem that is encountered when attempting to include magnetically charged particles; their mass goes to infinity. This type of divergence is common in quantum field theories and they are known as "ultraviolet divergences". The issue arises when, after quantising a field theory in a Lorentz covariant way, physical quantities such as scattering amplitudes appear to diverge. Full details of this can be found in [3], but a basic outline of the problem is as follows: Many physical quantities in quantum field theories (for example scattering amplitudes) involve integrals that are taken over all energy scales. These integrals are found to diverge due to increasingly large contributions at high energy scales (or equivalently small length scales) - hence the name "ultraviolet". The solution to this problem starts by introducing a regulator to modify the calculations such that they produce finite results, except in the limit where the regulator disappears and the original quantity is recovered. Once we have this regularisation in place, the next step is to introduce a renormali-sation scheme, where the divergences are absorbed into the parameters of the theory. The result of this is that when taking the limit where the regulator is removed, while these bare parameters will now diverge, the physical quantities remain finite. However, it is not always possible to use this procedure to renormalise all the quantities in a quantum field theory. The most well-known case of a non-renormalisable theory is gravity, and it is for this reason that creating a quantum theory of gravity has proven so difficult. In the case of QED without magnetic monopoles, the theory is renormalisable. With the addition of monopoles there is now an additional quantity - the monopole mass - which needs to be renormalised, but there are no longer enough parameters to absorb all the infinities; even after renormalisation the monopole mass is still infinite. There are, however, ways to resolve this. If we treat the theory as an effective theory valid only at low energies then the high energy "cut-off" will act as a regulator that stops the divergence. As will

be seen in the next chapter, lattice field theory provides one such regulator, allowing monopoles to exist in lattice QED.

2.2.2 't Hooft-Polyakov Monopoles

Although the monopole mass is found to be infinite when monopoles are included in QED, this is not the case when the U(1) QED theory emerges as the effective theory at low enough energies after symmetry breaking from a larger group. In fact, as originally found by 't Hooft [4] and Polyakov [5], monopole solutions inevitably exist for all Grand Unified Theories having U(1) QED emerge as a subgroup of the GUT group. Furthermore, whereas in the case of Dirac monopoles the vector potential contains a singularity, the monopole solutions for 't Hooft-Polyakov can be entirely smooth. This is because the "winding" of the U(1) phase around a loop must discontinuously jump from, for example, 2π when the loop is around Dirac string to 0 as the loop is moved past the end of the string, but for the larger group within which the U(1) is embedded, it is possible for this to be done continuously.

The simplest example consists of breaking the SU(2) symmetry. The Lagrangian density is given by

$$\mathcal{L} = -\frac{1}{4}F^a_{\mu\nu}F^{\mu\nu\,a} + \frac{1}{2}D_\mu\Phi^a D^\mu\Phi^a - V(\Phi), \tag{2.13}$$

where Φ^a is the Higgs field with a running over 1 to 3, $F^a_{\mu\nu}$ and D_μ are the SU(2) field strength tensor and covariant derivative respectively, and the potential $V(\Phi)$ is given by

$$V(\Phi) = \frac{1}{8}\lambda(\Phi^a\Phi^a - v^2)^2. \tag{2.14}$$

The vacuum solution has non-zero value for the Higgs field, but only specifies its magnitude as v, leaving a sphere of degenerate solutions corresponding to the direction of the Higgs field. The theory's SU(2) symmetry is therefore spontaneously broken in the vacuum state by the required choice of this direction; the remaining unbroken symmetry is the U(1) symmetry which can be identified with the emergence of QED. This vacuum solution allows the direction of the Higgs field to be chosen arbitrarily, and can vary with position in space. It is therefore possible to imagine a "hedgehog" solution where the direction of the Higgs field at a point $\mathbf{r}$ in space is aligned with $\mathbf{r}$, i.e $\Phi(\mathbf{r}) = f(r)\hat{\mathbf{r}}$. This means that at the origin the Higgs field must be zero, $f(0) = 0$, and hence this is not exactly the vacuum solution. At every other point the Higgs vector points away

from the origin. Note that the Higgs field is really a vector in an internal space, but since it is a three component vector, it is convenient in this case to think of the Higgs field as a vector field in terms of its position in real space. If we choose the magnitude of the Higgs field to be a smooth function which is zero at the origin, but quickly tends towards the vacuum expectation value v away from the origin, then this solution is "almost" a vacuum solution, and at large distances will appear as such. It will therefore look at large distances as if the SU(2) symmetry is broken with the U(1) QED emerging. However, close to the origin the solution deviates from the vacuum, suggesting a localised packet of energy, i.e. a particle. We identify this particle as a monopole as it turns out that this solution gives a magnetic field around the origin that has the exact form of a magnetic monopole, with charge consistent with the quantisation from Dirac monopoles. In this case the charge is found to be twice the minimum non-zero magnetic charge allowed, however different GUTs have solutions with the other values allowed by the quantisation condition (2.12).

Due to their topology, solutions of this type cannot be continuously transformed into the vacuum solution, and are a type of "topological defect". This also means that they are stable solutions and so 't Hooft-Polyakov monopoles are stable particles. In fact, it has been shown that such topologically non-trivial solutions exist in *all* theories where a gauge symmetry based on a simple Lie group is broken via the Higgs mechanism leaving a U(1) gauge symmetry, including all GUTs.

Unlike the Dirac monopole solutions in QED, the mass of 't Hooft-Polyakov monopoles is actually finite, with the mass scale close to the scale of the GUT at which the symmetry breaking occurs. For GUTs that aim to unify the forces of the Standard Model, this is of the order $\sim 10^{16}$ GeV, and monopoles are expected to have a mass around $10^{17} - 10^{18}$ GeV [6]. This is far beyond the mass of any particles that could be observed in collider experiments, for example, but this does not preclude the existence of monopoles of lighter mass, which could be observed in accelerator experiments. Monopoles of a mass beyond the reach of such experiments, could still have been created during the very hot early stages of the universe. If this was the case, then since they are stable particles we would expect that they would still exist in the universe. In fact, estimates of what the monopole density should be today predict a very large number of monopoles, which is not observed to be the case [7]. This problem lead to the suggestion of cosmological inflation [8], which has proven to be a highly successful theoretical concept, providing explanations for a number of other cosmological problems. As such, this suggests that monopoles could still exist as physical particles, and searches for experimental evidence of their existence have been carried out in a number of areas.

2.3   Searches for Monopoles in the Physical World

Despite the strong theoretical arguments for their existence, there has so far been no experimental evidence of magnetic monopoles. This is despite efforts to directly observe monopoles in cosmic rays, bound in matter, or produced in accelerators, and to indirectly observe their presence through their influence on astrophysical processes. The failure of these searches to find monopoles or observe their effects provides physical bounds on the properties of monopoles that could exist. For a more detailed discussion of this area see [6, 9]. The main techniques and results are summarised as follows; references for all of these can found in [6].

The induction method, used in searches for monopoles directly in cosmic rays, matter which has absorbed cosmic rays over long time periods, or matter removed from collider experiments, consists of identifying magnetic charges by the current that would be induced by the charge passing through a superconducting ring. Another method for measuring monopoles from cosmic rays or in colliders is to measure the tracks of the particles, where the electromagnetic energy loss of magnetically charged particles with the lowest allowed magnetic charge would be much larger than that of electrically charged particles with the lowest electric charge. In colliders, searches for monopoles have also been carried out by looking for their characteristic path in a magnetic field, distinct from the usual helical path of an electrically charged particle.

Searches have been attempted to find monopoles bound in matter exposed to cosmic rays over millions of years, using moon rock, meteorites and sea water; with no monopoles found in these attempts this gives an upper bound of $\sim 10^{-29}$ monopoles per nucleon. Searching for monopoles directly in cosmic rays has also been attempted, but again with no confirmed monopole observations. Bounds on the monopole flux from various experiments of this type are given in Figure 1. Although GUT monopoles are well out of reach of collider experiments due to their mass, it is possible that monopoles could exist with a lower mass but above the electroweak scale of around 100 GeV. Searches at colliders have so far excluded monopoles of mass less than around ~ 1 TeV. The most significant limits coming from the ATLAS experiment. A new experiment, MoEDAL, has recently been deployed at the Large Hadron Collider with the main aim to search for magnetic monopoles. Figure 2 shows a summary of the bounds placed on monopole production cross sections, from a number of collider experiments with collisions at different centre of mass energies. Indirectly detecting the existence of higher mass monopoles through the effects of virtual monopole-antimonopole pairs in high energy interactions at colliders has also been attempted, but the theoretical cal-

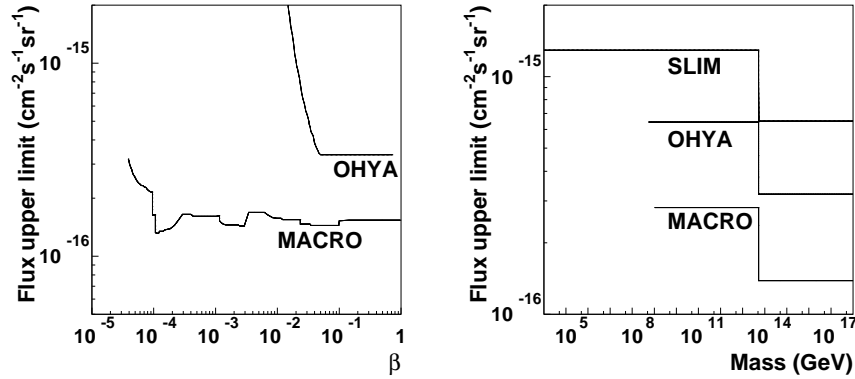culations used in these analyses are less reliable, giving more uncertain results than from direct searches.

Figure 1: Upper bounds on the flux of GUT monopoles as a function of their speed β and of the flux of monopoles as a function of their mass for $\beta > 0.05$ [6].
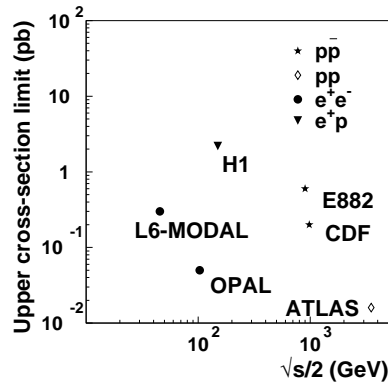
Figure 2: Upper bounds placed on monopole production cross sections for various centre of mass collision energies [6].

It is also possible to probe the existence of monopoles by looking for indirect evidence from their expected effect on various physical processes. One such process is nucleon decay; it is possible that GUT monopoles could catalyse the decay of the proton due to the GUT's symmetry being unbroken within the monopole removing the potential barrier which would otherwise exist for the decay. A recent result from an experiment of this type was from Super-Kamiokande which placed an upper bound on the monopole flux of $6.3 \times 10^{-24} \left(\frac{\beta}{10^{-3}} \right)^2$ cm^{-2}sr^{-1}s^{-1}, where β is the speed of the monopole. Another bound, known as the *Parker bound*, can be placed on the flux of monopoles by considering that they would be expected to drain energy from magnetic fields of galaxies or clusters of galaxies. Given the size of the magnetic fields observed, the requirement that the monopole flux

drains energy from the magnetic field slowly compared to the rate at which it can be regenerated gives the upper bound on the flux as $10^{-15}\text{cm}^{-2}\text{sr}^{-1}\text{s}^{-1}$ for monopoles of mass less then $\sim 10^{17}$ GeV, where their motion is not dominated by gravitational forces. A similar bound can also be obtained by considering the total mass of monopoles in the universe. Monopoles could form the observed dark matter of the universe, and from the dark matter density the upper bound, for monopoles of mass M with average speed v, is found to be $1.3 \times 10^{-17} \dfrac{10^{17}\text{GeV}}{M} \dfrac{v}{10^{-3}c} \text{cm}^{-2}\text{sr}^{-1}\text{s}^{-1}$.

3 Lattice Field Theory

3.1 The Motivation for Lattice Field Theory

There are a number of reasons for the interest that has arisen over the past few decades in Lattice field theories - the formulation of quantum field theories on a discrete spacetime lattice. The concept was originally proposed by Wegner as a locally gauge invariant generalisation of the Ising model [10], however it was Wilson's formulation, introduced in investigations into confinement [11], that laid the foundations for the lattice field theories of gauge theories that have been investigated since. In Wilson's paper the lattice gauge theory is used as a method of regularisation; a step in the solution to the problem of ultraviolet divergences previously discussed in Section 2.2.1.

There are various different techniques used for both regularisation and renormalisation. Examples of methods for regularisation include taking a high energy cut-off, Λ, recovering the original theory as $\Lambda \to \infty$, or taking the spacetime to be of dimension $d = 4 - \epsilon$, with the original theory recovered as $\epsilon \to 0$. Lattice field theory was introduced as an alternative method for regularisation where calculations are instead regularised by introducing a minimum length scale. This is achieved by formulating the quantum theory on a discrete lattice in spacetime, with the physical theory being recovered in the limit where the lattice spacing between two spacetime points is taken to zero. This was the original motivation for formulating quantum field theories on a lattice, yet there are also advantages to using lattices over other techniques. Quantities in quantum field theory are usually calculated using perturbation theory; a series of Feynman diagrams are computed, expanding in powers of the coupling constant. This works well, and has been very successfully used in predicting physical quantities, for cases where the coupling constant is small such as quantum electrodynamics, and quantum chromodynamics (QCD) at high energies. It is less suited, however, to theories with large coupling constants like QCD at low energies. Calculations on a lattice provide a way to produce genuinely non-perturbative results; indeed, significant advances in understanding aspects of QCD have emerged from research in lattice QCD. In the case of studying monopoles, the Dirac quantisation condition (2.12) results in a magnetic coupling constant which is large precisely when the electric coupling constant is small. Furthermore the topological nature of the monopole solution means that it is not just a perturbation of the vacuum. This make it difficult to study perturbatively, and so non-perturbative methods such as lattice field theory is required. From a purely practical point of view, lattice field theory also has the advantage that the discreteness

of the lattice spacetime lends itself well to performing computations; as will be seen later, the
calculations in lattice field theory bear a striking resemblance to those in statistical mechanics,
allowing the computational techniques developed for calculations in that field to also be used for
calculations in lattice field theory. Finally, for gauge theories there is the appeal that the lattice
gauge theory retains manifest gauge invariance, whereas other methods generally require gauge
fixing until the gauge invariance is recovered after renormalisation.

3.2   Quantum Path Integrals

The path integral formulation of quantum field theory is the one that is of most interest for lattice
field theory. This will be briefly reviewed in this section, first as applied to a simple quantum
mechanical system with one degree of freedom, and then to scalar fields. Full details can be found
in [3].

3.2.1   Path Integrals in Quantum Mechanics

Consider a quantum system with a single degree of freedom, described by the Hamiltonian operator

$$\hat{H} = H[\hat{q}, \hat{p}] = \frac{\hat{p}^2}{2m} + V(\hat{q}). \tag{3.1}$$

In natural units, the time evolution of the system is described by the operator

$$\hat{U}(T) = e^{-iT\hat{H}}. \tag{3.2}$$

The amplitude for a particle to travel from point q_a to q_b in time T, can be represented as the
path integral

$$\langle q_b| \, \hat{U}(T) \, |q_a\rangle = \int_{q_a(x)}^{q_b(x)} \mathcal{D}q(t) \, e^{iS[q(t)]}, \tag{3.3}$$

where $\int_{q_a(x)}^{q_b(x)} \mathcal{D}q(t)$ represents a functional integral over all functions $q(t)$ (i.e. all paths) where
$q(0) = q_a$ and $q(T) = q_b$, and $S[q(t)]$ is the action of the system,

$$S[q(t)] = \int dt \, L[q(t), \dot{q}(t)], \tag{3.4}$$

where L is the Lagrangian corresponding to the Hamiltonian H. To define the path integration measure $\mathcal{D}q(t)$, we consider splitting the time interval T into N smaller intervals ϵ. By making the replacement $\hat{U}(T) = \hat{U}(\epsilon)^N$, inserting a complete set of states $\mathbf{1} = \int dq_k \, |q_k\rangle \, \langle q_k|$ between each $\hat{U}(\epsilon)$, and taking the limit $N \to \infty, \epsilon \to 0$, this gives

$$\int \mathcal{D}q(t) = \sqrt{\frac{m}{2\pi i\epsilon}} \prod_{k=0}^{N} \sqrt{\frac{m}{2\pi i\epsilon}} \int dq_k. \tag{3.5}$$

3.2.2   Scalar Field Theory

This path integral formulation generalises in a straightforward way to scalar field theory. We now have the Hamiltonian

$$\hat{H} = \int d^4x \left[\frac{1}{2}\hat{\pi}^2 + \frac{1}{2}\left(\frac{d\hat{\phi}}{dx}\right)^2 + V(\hat{\phi}) \right], \tag{3.6}$$

with the amplitude from field $\phi_a(\mathbf{x})$ to $\phi_b(\mathbf{x})$ in time T is given by

$$\langle\phi_b| \, \hat{U}(T) \, |\phi_a\rangle = \int \mathcal{D}\phi(x) \, e^{iS[\phi(x)]}, \tag{3.7}$$

where the functional integral $\int \mathcal{D}\phi(x)$ is now over all Minkowski spacetime functions $\phi(x)$ satisfying $\phi(0, \mathbf{x}) = \phi_a(\mathbf{x})$ and $\phi(T, \mathbf{x}) = \phi_b(\mathbf{x})$, and the action is now given by $S = \int d^4x \, \mathcal{L}$ where $\mathcal{L}$ is the Lagrangian density

$$\mathcal{L} = \frac{1}{2}\partial_\mu\phi\partial^\nu\phi - V(\phi). \tag{3.8}$$

Repeating a similar procedure that derives the path integral (3.7), time ordered n-point functions are found to be given by

$$\langle\phi_b| \, T\hat{\phi}(x_1^{\mu_1})\hat{\phi}(x_2^{\mu_2})\ldots\hat{\phi}(x_n^{\mu_n}) \, |\phi_a\rangle = \int \mathcal{D}\phi(x) \, e^{iS} \phi(x_1^{\mu_1})\phi(x_2^{\mu_2})\ldots\phi(x_n^{\mu_n}). \tag{3.9}$$

By considering then the time evolution of a state $|\phi\rangle$ at time $-T$, for $T \to (1 - i\epsilon)T$ and $T \to \infty$, and decomposing $|\phi\rangle$ into energy eigenstates $|n\rangle$ satisfying $\hat{H}\,|n\rangle = E_n\,|n\rangle$, and rearranging to get an expression for $|0\rangle$, the vacuum expectation value $\langle\hat{\mathcal{O}}\rangle$ of an operator $\hat{\mathcal{O}}[\phi]$ is found to be

$$\langle 0| \, T\hat{\mathcal{O}}[\hat{\phi}] \, |0\rangle = \lim_{T \to \infty} \frac{e^{2\epsilon E_0 T}}{\langle\phi_b|0\rangle \, \langle 0|\phi_a\rangle} \int \mathcal{D}\phi(x) \, e^{iS}\mathcal{O}[\phi]. \tag{3.10}$$

Then, since this is true also for the identity, $\mathbf{1}$, we have

$$\mathbf{1} = \langle 0|0 \rangle = \int \mathcal{D}\phi(x)\, e^{iS}, \tag{3.11}$$

and so

$$\langle 0 | T\hat{\mathcal{O}}[\hat{\phi}] | 0 \rangle = \frac{\int \mathcal{D}\phi(x)\, e^{iS} \mathcal{O}[\phi]}{\int \mathcal{D}\phi(x)\, e^{iS}}. \tag{3.12}$$

It is worth noting here that if time is rotated to the imaginary axis via a Wick rotation,

$$t \to it, \tag{3.13}$$

so that we are working in Euclidean space, these integrals then become real, bounded, and more convenient to work with. In most cases the results produced will still stand, while in other cases a rotation back to real time can be performed to obtain the correct value. After the rotation (3.13), Equations (3.12) and (3.11) become

$$\langle 0|0 \rangle = \int \mathcal{D}\phi(x)\, e^{-S} \tag{3.14}$$

$$\langle 0 | T\hat{\mathcal{O}}[\hat{\phi}] | 0 \rangle = \frac{\int \mathcal{D}\phi(x)\, e^{-S} \mathcal{O}[\phi]}{\int \mathcal{D}\phi(x)\, e^{-S}}, \tag{3.15}$$

where S now refers to the Euclidean action

$$S[\phi(x)] = \int d^4x \left[\frac{1}{2}(\partial_0 \phi)^2 + \frac{1}{2}(\partial_i \phi)^2 + V(\phi) \right]. \tag{3.16}$$

In this form, the analogy with statistical mechanics is clear. Equation (3.14) has the form of the partition function and Equation (3.15) has the form of an observable in a statistical mechanical system. This demonstrates how the techniques of statistical mechanics can be applied to problems in quantum field theories; in particular the computational methods can be used with lattice field theory.

3.2.3   Gauge Theories

The theories that appear to describe the physical world exhibit local gauge invariance; the action $S[\psi(x), \bar{\psi}(x)]$ is invariant under the local gauge transformation

$$
\begin{aligned}
\psi(x) \rightarrow \psi'(x) &= G(x)\psi(x) \\
\bar{\psi}(x) \rightarrow \bar{\psi}'(x) &= \bar{\psi}(x)G^{-1}(x),
\end{aligned}
\tag{3.17}
$$

where $G(x)$ is an element of the gauge group $\mathcal{G}$ which varies in spacetime. Here the field $\psi(x)$ transforms under some representation of $\mathcal{G}$ and $\bar{\psi}(x)$ transforms in the conjugate representation to $\psi(x)$.

To construct such a theory, the gauge fields $A_\mu(x) = A_\mu^a t^a$ are introduced, where t^a are the generators of G satisfying $[t^a, t^b] = i f^{abc} t^c$ for the group's structure constants f^{abc}. The gauge fields transform in the adjoint representation of $\mathcal{G}$ as

$$
A_\mu(x) \rightarrow A'_\mu(x) = G(x)A_\mu(x)G^{-1}(x) + \frac{i}{g}G(x)\partial_\mu G^{-1}(x),
\tag{3.18}
$$

This gauge field is used in the covariant derivative D_μ of ψ, which replaces the usual derivative ∂_μ due to objects such as $\partial_\mu \psi(x)$ not being gauge invariant,

$$
D_\mu \psi = (\partial_\mu + ig A_\mu)\psi.
\tag{3.19}
$$

The field strength tensor is also introduced as

$$
F_{\mu\nu}(x) = \partial_\mu A_\nu(x) - \partial_\nu A_\mu(x) + ig[A_\mu(x), A_\nu(x)],
\tag{3.20}
$$

or, in terms of components,

$$
F_{\mu\nu}^a(x) = \partial_\mu A_\nu^a(x) - \partial_\nu A_\mu^a(x) + ig f^{abc} A_\mu^b(x) A_\nu^c(x).
\tag{3.21}
$$

We are now in a position to construct a number of gauge invariant terms for the action. For example, the QCD action with the gauge group SU(3) is given by $S[\psi, \bar{\psi}, A_\mu] = \int d^4x \, \mathcal{L}[\psi, \bar{\psi}, A_\mu]$

with Lagrangian density

$$\mathcal{L}[\psi, \bar{\psi}, A_\mu] = -\frac{1}{2}\operatorname{Tr}[F_{\mu\nu}F^{\mu\nu}] + \bar{\psi}(i\gamma^\mu D_\mu - m)\psi. \tag{3.22}$$

In fact, the Yang-Mills term $\operatorname{Tr}[F_{\mu\nu}F^{\mu\nu}]$ alone is a gauge invariant object, and so it is possible to construct a pure gauge field theory comprising only of the gauge field A_μ.

As with the scalar theory, expectation values of observables can be calculated using path integrals. After performing the rotation to imaginary time as before, the expression for these observables is

$$\langle 0| T\hat{\mathcal{O}}[\hat{A}_\mu, \hat{\psi}, \hat{\bar{\psi}}] |0\rangle = \frac{\displaystyle\int \mathcal{D}\psi(x)\mathcal{D}\bar{\psi}(x)\mathcal{D}A_\mu(x)\, e^{-S}\mathcal{O}[A_\mu, \psi, \bar{\psi}]}{\displaystyle\int \mathcal{D}\psi(x)\mathcal{D}\bar{\psi}(x)\mathcal{D}A_\mu(x)\, e^{-S}}. \tag{3.23}$$

Our gauge invariant path integral is now also over the group-valued gauge field $A_\mu(x)$. To obtain a proper meaning for the full integration measure for these gauge theories, $\mathcal{D}\psi\mathcal{D}\bar{\psi}\mathcal{D}A_\mu$, or for scalar field theories, $\mathcal{D}\phi$, lattice regularisation will need to be introduced.

3.3   Lattice Regularisation

In Section 3.2.1 it was seen that for the path integral of a quantum mechanical system (3.3) with a single degree of freedom, it was necessary to split time into a finite number of discrete slices in order to formally define the integration measure (3.5). For a quantum field theory such as the scalar theory described in Section 3.2.2, or the gauge theories described in Section 3.2.3, we again give well-defined mathematical meaning to the path integrals by discretisation; here though the whole of spacetime is discretised onto a lattice. This process is called lattice regularisation and results in a lattice field theory.

The lattice regularisation takes place after the Wick rotation (3.13), so that we have a Euclidean spacetime and use the Euclidean form of the theory's action, given by Equation (3.16) for the scalar theory. The continuum of spacetime x^μ is replaced by a finite lattice of points separated by the lattice spacing a, with $N = \dfrac{L}{a}$ points in each direction, such that $x_\mu = an_\mu$ for $n_\mu = 0, 1, \ldots, N = 1$. The field is now only defined at these points, $\phi(x) \to \phi_x$, and derivatives are replaced by finite differences

$$\partial_\mu \phi(x) \to \partial_\mu \phi_x \equiv \frac{1}{a}(\phi_{x+a\hat{\mu}} - \phi_x). \tag{3.24}$$

Spacetime integrals are then replaced with sums

$$\int d^4x \to a^4 \sum_{n_0=0}^{N-1} \cdots \sum_{n_3=0}^{N-1} \equiv a^4 \sum_x, \qquad (3.25)$$

and the path integral then becomes a usual multiple integral

$$\int \mathcal{D}\phi(x) \to \prod_{n_0=0}^{N-1} \cdots \prod_{n_3=0}^{N-1} \left(\int_{-\infty}^{\infty} d\phi_x \right) \equiv \prod_x \left(\int_{-\infty}^{\infty} d\phi_x \right). \qquad (3.26)$$

This is already enough to construct a lattice field theory and start to perform calculations. The partition function is given by

$$Z = \int \prod_x d\phi_x \, e^{-S[\phi]}, \qquad (3.27)$$

where the discretised action is given by

$$S[\phi] = a^4 \sum_x \left[\frac{1}{2}(\partial_0\phi)^2 + \frac{1}{2}(\partial_i\phi)^2 + V(\phi) \right]. \qquad (3.28)$$

Physical observables can then be calculated as

$$\langle \hat{\mathcal{O}} \rangle = \frac{1}{Z} \int \prod_x d\phi_x \, \mathcal{O}[\phi] \, e^{-S[\phi]}. \qquad (3.29)$$

Finally, to recover the original continuum theory, the limits $N \to \infty, a \to 0$ must be taken. While computations can only be performed on a finite lattice, many properties of the lattice theory are expected to continue into the continuum theory. As such, lattice field theories provide a convenient tool to investigate the corresponding continuum theories.

The theory described above describes the lattice formulation of a scalar field theory, but it is gauge theories that have been enormously successful in describing the particle physics observed in the real world, and these are the theories where studying the lattice formulations have provided real insights into understanding aspects of the theories that are otherwise inaccessible.

3.4   Formulation of Gauge Theories on a Lattice

In order to see how the gauge theories of Section 3.2.3 can be formulated on a spacetime lattice - in particular how the lattice equivalents of spacetime derivatives (3.24) can be replaced with suitable

covariant derivatives - it is useful to introduce the transport operator. This operator, as applied to a field at a point x parallel transports the field to the point $x + dx$, and takes the form

$$e^{igA_\mu dx^\mu}. \tag{3.30}$$

This is the geometrical reason for the above form of the covariant derivative (3.19), since

$$
\begin{aligned}
\partial_\mu \left(e^{igA_\nu dx^\nu} \psi(x) \right) &= \partial_\mu \left(\psi(x) + igA_\nu dx^\nu \psi(x) + \mathcal{O}((dx^\nu)^2) \right) \\
&= \partial_\mu \psi(x) + igA_\mu \psi(x) + \mathcal{O}(dx^\nu) \\
&= D_\mu \psi(x) + \mathcal{O}(dx^\nu),
\end{aligned}
\tag{3.31}
$$

and so the derivative of the field at $x + dx^\nu$ - equal to the derivative of the field at x transported along the infinitesimal distance dx^ν - is equal to the covariant derivative of the field at x. The transport operator transforms under the gauge transformation (3.17) as

$$e^{igA_\mu dx^\mu} \to G(x) e^{igA_\mu dx^\mu} G^{-1}(x + dx), \tag{3.32}$$

so that the products of fields at different points can be made gauge invariant

$$
\begin{aligned}
&\bar{\psi}(x) e^{igA_\mu dx^\mu} \psi(x + dx) \\
&\to \bar{\psi}(x) G^{-1}(x) G(x) e^{igA_\mu dx^\mu} G^{-1}(x + dx) G(x + dx) \psi(x + dx) \\
&= \bar{\psi}(x) e^{igA_\mu dx^\mu} \psi(x + dx).
\end{aligned}
\tag{3.33}
$$

On the lattice, we have the gauge transformations

$$
\begin{aligned}
\psi_x &\to G_x \psi_x \\
\bar{\psi}_x &\to \bar{\psi}_x G_x^{-1}.
\end{aligned}
\tag{3.34}
$$

The gauge field on the lattice can therefore be represented by a discretised version of the transport operator, given by the link variables, $U_{x,x+\hat{\mu}} \in \mathcal{G}$, between two neighbouring points on the lattice, x and $x + a\hat{\mu}$, where we use the notation

$$
\begin{aligned}
U_{\mu,x} &= U_{x,x+\hat{\mu}} \\
U_{\mu,x}^{-1} &= U_{x+\hat{\mu},x}.
\end{aligned}
\tag{3.35}
$$

These are related to the continuum gauge field by

$$U_{\mu,x} = e^{ig\alpha_{\mu,x}},$$ (3.36)

where $\alpha_{\mu,x}$ is the discrete replacement for the gauge field, $A_\mu(x) \to \frac{1}{a}\alpha_{\mu,x}$. As required, the links transform under a gauge transformation as

$$U_{\mu,x} = G_x U_{\mu,x} G_{x+\hat{\mu}}^{-1}.$$ (3.37)

The covariant derivative is then replaced with the discretised version

$$D_\mu \psi(x) \to D_\mu \psi_x = \frac{1}{a}(U_{\mu,x}\psi_{x+a\hat{\mu}} - \psi_x).$$ (3.38)

The transport operator above can also be used to define the parallel transport along a path γ from pont x_1 to x_2

$$U_\gamma = \mathrm{P}\, e^{ig \int_\gamma A_\mu dx^\mu},$$ (3.39)

which will transform as

$$U_\gamma \to U'_\gamma = G(x_1) U_\gamma G^{-1}(x_2).$$ (3.40)

For a closed loop λ, starting and finishing at point x, this becomes

$$U_\lambda \to U'_\lambda = G(x) U_\gamma G^{-1}(x),$$ (3.41)

and so gauge invariant objects known as Wilson loops can be created from the trace of U_λ. In fact, the field strength tensor can be seen to be such an object; geometrically it represents the parallel transport around the infinitesimal square with edges, dx^μ and dx^ν, given by

$$e^{igF_{\mu\nu}dx^\mu dx^\nu}.$$ (3.42)

The discrete form of this is therefore the ordered product of the links around a square of unit one, known as a plaquette, giving the gauge invariant plaquette transport operator

$$U_{\mu\nu,x} = U_{\mu,x} U_{\nu,x+\hat{\mu}} U_{\mu,x+\hat{\nu}}^{-1} U_{\nu,x}^{-1}.$$ (3.43)

As the continuum limit is approached, combining the exponentials in the link variables for small a using the Baker-Campbell-Hausdorff formula, this becomes

$$U_{\mu\nu,x} = e^{iga^2 F_{\mu\nu,x} + \mathcal{O}(a^3)}. \tag{3.44}$$

where we have used the discretised form of the field tensor, which after replacing the usual derivatives with finite differences has the form

$$F_{\mu\nu}(x) \to F_{\mu\nu,x} = \frac{1}{a^2}(\alpha_{\nu,x+\hat\mu} - \alpha_{\nu,x} - \alpha_{\mu,x+\hat\nu} + \alpha_{\mu,x}). \tag{3.45}$$

Using these gauge invariant objects it is now possible to construct the action for a lattice gauge theory. However, a given continuum action will not generally specify a unique action for the lattice theory; there will be a large class of possible actions with the same continuum limit.

If we have Yang-Mills theory, with Lagrangian density

$$\mathcal{L} = \frac{1}{4} F_{\mu\nu}^a F^{\mu\nu\,a}, \tag{3.46}$$

then one possibility for the action is Wilson's action

$$S[U_{\mu\nu,x}] = \sum_x \sum_{\mu<\nu} \frac{\beta}{N}(1 - \mathrm{Re}[\mathrm{Tr}\,U_{\mu\nu,x}]), \tag{3.47}$$

where β is a numerical constant proportional to $\dfrac{1}{g^2}$ which depends on the normalisation convention used for the group $\mathcal{G}$. From now on we will work only with these pure gauge theories due to difficulties that arise when dealing with fermions on the lattice[2].

For $\mathcal{G} = \mathrm{SU}(N)$ or $\mathcal{G} = \mathrm{U}(1)$, with $\beta = \dfrac{2N}{g^2}$ or $\beta = \dfrac{1}{g^2}$ respectively, expanding the exponential in Equation (3.44) for small a, the action becomes

$$S[U_{\mu\nu,x}] = \frac{a^4}{4} \sum_x F_{\mu\nu,x}^a F_x^{\mu\nu\,a} + \mathcal{O}(a^2), \tag{3.48}$$

giving the correct continuum limit (3.46).

---

[2]For a discussion of these problems and how to deal with them, see [12].

The expressions for the partition function and observables now become

$$Z = \int dU \, e^{-S[U]} \tag{3.49}$$

$$\langle \hat{\mathcal{O}} \rangle = \frac{1}{Z} \int dU \, \mathcal{O}[U] e^{-S[U]}, \tag{3.50}$$

where

$$dU = \prod_x \prod_\mu dU_{\mu,x}. \tag{3.51}$$

This integration measure is the unique gauge invariant measure over the entire group manifold, and for compact groups this is finite due to the finite group volume and so the integral for the partition function (3.49) is well defined. In any case, the factor obtained due to the group's volume will cancel in the expression for observables (3.50) due to the partition function in the denominator.

In principle, for the well-defined integrals of a compact group, calculations of these quantities could be computed by brute force, performing a multi-dimensional numerical integration over the entire configuration space. But to do this in practice would take an intractable amount of time due to the sheer number of different field configurations on a lattice of any reasonable size. This is where the Monte-Carlo techniques developed for statistical mechanics become invaluable, and will be discussed in more detail in Chapter 4.

3.5   Compact U(1) Lattice Gauge Theory

The particular theory that will be investigated here is the pure compact U(1) lattice gauge theory. Taking $\mathcal{G} = \mathrm{U}(1)$, Wilson's action (3.47) reduces to

$$S[\theta_{\mu\nu,x}] = \beta \sum_{\mu<\nu} \sum_x \left[1 - \cos(\theta_{\mu\nu,x})\right], \tag{3.52}$$

where $\beta = \dfrac{1}{e^2}$ and we take as our dynamical parameters the plaquette flux angles $\theta_{\mu\nu,x} \in [-4\pi, 4\pi]$, defined as

$$U_{\mu\nu,x} = e^{i\theta_{\mu\nu}} \tag{3.53}$$

$$\theta_{\mu\nu,x} = ea^2 F_{\mu\nu,x} = \theta_{\mu,x} + \theta_{\nu,x+\hat{\mu}} - \theta_{\mu,x+\hat{\nu}} - \theta_{\nu,x}, \tag{3.54}$$

for link angles $\theta_{\mu,x} \in [-\pi, \pi]$, which differ from the $\alpha_{\mu,x}$ introduced in Equation (3.35) only by a factor of the coupling constant g, which has been absorbed into the link angles and plaquette angles for convenience. The gauge transformations of the theory take the form

$$G_x = e^{i\omega_x}, \tag{3.55}$$

and so the link angles transform as

$$\theta_{\mu,x} \to \theta'_{\mu,x} = \theta_{\mu,x} + \omega_{x+\hat{\mu}} - \omega_x \quad \text{mod } 2\pi. \tag{3.56}$$

In the action (3.52) the defining representation of U(1) has been used, and the theory is known as compact U(1). We can also sum over the other representations ρ_r of U(1) in the action as a Fourier series

$$S[\theta_{\mu\nu,x}] = \sum_r \beta_r \sum_{\mu<\nu} \sum_x \cos(r\theta_{\mu\nu,x}) + \text{constant}, \tag{3.57}$$

giving, for example, the extended Wilson action

$$S[\theta\mu\nu, x] = \sum_{\mu<\nu} \sum_x \left[\beta \cos(\theta_{\mu\nu,x}) + \gamma \cos(2P_{\mu\nu,x}) \right], \tag{3.58}$$

or we could have chosen the Villain action

$$S[\theta_{\mu\nu,x}] = \sum_{\mu<\nu} \sum_x - \ln \sum_{k=-\infty}^{\infty} e^{-\frac{\beta}{2}(\theta_{\mu\nu,x}+2\pi k)^2}. \tag{3.59}$$

These are again actions for compact U(1), however it is also possible to have a non-compact U(1) lattice gauge theory; appropriate choices of the values of β_r produce the action

$$S[\theta_{\mu\nu,x}] = \beta \sum_{\mu<\nu} \sum_x \theta_{\mu\nu,x}. \tag{3.60}$$

where the gauge transformations no longer involve the mod 2π in Equation (3.56), and the group is really $\mathcal{G} = \mathbb{R}$.

It is the compact form of the theory that we will be using, since compact U(1) contains monopoles while non-compact U(1) does not.

3.5.1   Monopoles in Compact U(1)

We will be using the definition of a magnetic monopole on a lattice introduced in [13]. To find magnetic charges on the lattice the magnetic flux out of a cube is determined, giving the magnetic charge within the cube via Gauss's Law. The magnetic field in the lattice is related to the plaquettes as

$$\mathbf{B}_i = \frac{1}{2}\epsilon_{ijk}\theta_{jk,x}. \tag{3.61}$$

However, the physical part of these plaquettes is really the plaquette mod 2π. We therefore define the physical flux, $\bar{\theta}_{\mu\nu} \in [-\pi, \pi]$ as

$$\bar{\theta}_{\mu\nu,x} = \theta_{\mu\nu} + 2\pi n_{\mu\nu,x}, \tag{3.62}$$

where $n_{\mu\nu} \in \{0, \pm 1, \pm 2\}$ corresponds to the number of Dirac strings passing through the plaquette. This is because a Dirac string causes the value of the gauge field to wind once around 2π, as described in Section 2.2.1, and this corresponds to the plaquette angle also winding round 2π. The lattice monopole number within a surface, equivalent to $\nabla \cdot \mathbf{B}$ in the continuum, is therefore given as

$$2\pi M_x = \sum_{\text{boxes}} \nabla_i \epsilon_{ijk} \bar{\theta}_{jk,x} \tag{3.63}$$

$$= \sum_{\text{boxes}} \epsilon_{ijk}(\bar{\theta}_{jk,x+\hat{\mathbf{i}}} - \bar{\theta}_{jk,x}) \tag{3.64}$$

$$= 2\pi \sum_{\text{boxes}} \epsilon_{ijk}(n_{jk,x+\hat{\mathbf{i}}} - n_{jk,x}). \tag{3.65}$$

In four dimensions, this corresponds to the monopole's flux through the time dimension, with the point-like charges in 3-dimensions becoming 1-d strings in 4 dimensions, corresponding to the worldlines of monopoles. We can therefore define the monopole flux as

$$M_{\rho,x} = \frac{1}{2\pi}\epsilon_{\rho\sigma\mu\nu}\nabla_\sigma\bar{\theta}_{\mu\nu,x} \tag{3.66}$$

$$= \frac{1}{2\pi}\epsilon_{\rho\sigma\mu\nu}(\bar{\theta}_{\mu\nu,x+\hat{\sigma}} - \bar{\theta}_{\mu\nu,x}) \tag{3.67}$$

$$= \epsilon_{\rho\sigma\mu\nu}(n_{\mu\nu,x+\hat{\sigma}} - n_{\mu\nu,x}). \tag{3.68}$$

Due to the quantisation of magnetic charge, the monopole number and flux are expected to be integers, and this is seen explicitly with the form in Equation (3.68). Due to the lattice regular-

isation, the mass of these monopoles remains finite, and we find that they do exist in the lattice simulations. The worldlines delineated by this flux form closed loops due to magnetic charge conservation, $\nabla_\mu M_\mu = 0$ (except in the case where the total magnetic charge in the lattice is forced to be non-zero by an appropriate choice of boundary conditions, as will be discussed in Section 4.3.2).

Since standard QED does not contain monopoles, it is expected that as the continuum limit of the lattice theory is taken these monopoles will disappear. Indeed, this does happen and as the lattice spacing is increased the monopoles become suppressed as their mass effectively goes to infinity, exactly as expected. However, compact QED without monopoles has been studied on finite lattices by suppressing them via the action [14]; by adding a term to the action proportional to $|M_\mu|$,

$$S[\theta_{\mu\nu,x}] = \sum_x \left(\beta \sum_{\mu<\nu} \theta_{\mu\nu,x} + \lambda \sum_\mu |M_{\mu,x}| \right), \tag{3.69}$$

and taking its coefficient λ to infinity, any lattice configurations which contain monopoles will be given a zero weighting in the path integral. The theory has also been studied with finite λ, but again usually to suppress monopoles [15]. However, if the value of λ is taken to be negative, monopoles are enhanced rather than suppressed, and so this term could provide a way to keep the monopole mass small even as the lattice spacing is reduced as the continuum limit is taken. For this reason, we have chosen this action to investigate the monopole's properties on the lattice.

3.5.2   Confinement and the Phase Structure of Compact U(1)

One of the great successes of lattice gauge theories has been in understanding the phenomenon of confinement. It was this subject that was addressed by Wilson's paper which laid the foundations of lattice gauge theories [11]. The monopoles in lattice gauge theories turn out to be fundamental to the mechanism known as "dual superconductivity", proposed by Mandelstam [16] and 't Hooft [17], which attempts to explain confinement via electric-magnetic duality as a dual Meissner effect. For full details on this topic see [18], but a brief outline is as follows. If a phase exists where a condensate of monopoles form, then they can act in analogy to the Cooper pairs of superconductivity. The dual Meissner effect then attempts to eliminate the electric charge, and this is achieved by restricting the charged particles and anti-particles to as small a space as possible, with a thin flux tube between them. If the particles are separated, the flux tube extends between them, remaining thin, and so the energy increases linearly with the distance, as is the case in confinement. For QCD, where

confinement is observed in the physical world, it is the colour charge that is excluded by the dual Meissner effect, and quarks that are confined.

While confinement in the physical world is only observed in QCD, the compact U(1) lattice gauge theory does also exhibit a confinement phase [13] for $\beta > \beta_c$. This phase is characterised by the formation of a monopole condensate and the electric field is confined by the dual superconductivity mechanism [19]. For the Wilson action (3.52) the phase transition is at a critical value of around $\beta_c = 1.01$ and for the action with the monopole included, the critical value of β is found to decrease as λ is increased, due to the suppression of monopoles [15]. The transition was also found to change from being of second order at large enough λ and becomes first order with smaller λ, with the energy barrier between the two phases increasing as λ is decreased [29]. When λ is taken to infinity, the confined phase disappears altogether [14]. We will be attempting to investigate the properties of monopoles in the Coulomb phase $\beta > \beta_c$, but with negative values of λ to the reduce the monopole mass.

4 Numerical Simulations

4.1 Monte Carlo Methods

To measure the expectation value of an observable (3.50), we need some way of computing the multiple integrals. For discrete groups these integrals simply correspond to a finite sum over the group elements, and for continuous groups the integrals can be approximated by sums over a sufficiently dense set of points in the group manifold. For a lattice of side L, there are $4L^4$ link variables being integrated over, so if we attempted to compute such a sum with N possible values for each link variable, then we would have in total N^{4L^4} terms. Even for the smallest non-trivial group, $\mathbf{Z}_2$ on a modest lattice with $L = 8$ this is more than 10^{4932} terms; clearly this is not practical. However, due to the analogy with statistical mechanics noted at the end of Section 3.2.2, the methods developed for statistical mechanics can be used to reduce this sum to a manageable calculation.

Each term in this sum corresponds to a configuration U_n which is weighted by the factor $e^{-S[U_n]}$

$$\langle \mathcal{O} \rangle = \frac{1}{Z} \sum_n \mathcal{O}[U_n] e^{-S[U_n]}. \tag{4.1}$$

This weighting results in only a small subset of configurations providing any significant contribution to the expectation value (3.50). Taking a randomly selected ensemble of configurations, where the probability, P_n, of selecting a configuration, U_n, is proportional to its weight,

$$P_n = C e^{-S[U_n]} \tag{4.2}$$

then the mean of the observable over this ensemble will converge towards the exact result

$$\begin{aligned}
\lim_{N \to \infty} \frac{1}{N} \sum_{n=1}^{N} \mathcal{O}[U_n] &= \frac{\sum_n \mathcal{O}[U_n] P_n}{\sum_n P_n} \\
&= \frac{C \sum_n \mathcal{O}[U_n] e^{-S[U_n]}}{C \sum_n e^{-S[U_n]}} \\
&= \frac{1}{Z} \sum_n \mathcal{O}[U_n] e^{-S[U_n]}.
\end{aligned} \tag{4.3}$$

By using a method to efficiently pick ensembles from this probability distribution, the configurations which contribute most to the result will be included much more quickly than picking randomly

from a uniform distribution or simply summing over all configurations, and so the computation
will converge within a reasonable time.

4.2   The Metropolis Algorithm

The method that will be used to select configurations with probability proportional to their weights
is known as the Metropolis algorithm [20], a form of Markov chain Monte Carlo. This type of algo-
rithm works by taking some initial configuration, U_1, then repeatedly selecting new configurations
from a probability distribution dependant on the previous, $P(U_n \rightarrow U_{n+1})$. Then, the equilibrium
distribution of this Markov chain will equal $e^{-S[U]}$ if $P(U_n \rightarrow U_{n+1})$ satisfies

$$\frac{P(U_n \rightarrow U_{n+1})}{P(U_{n+1} \rightarrow U_n)} = \frac{e^{-S[U_{n+1}]}}{e^{-S[U_n]}}. \tag{4.4}$$

The Metropolis algorithm starts with U_1, and repeats the following steps

1. A proposed new configuration U_p is chosen from the current configuration U_n by a random
   process with probability $P_{\text{proposal}}(U_n \rightarrow U_p)$ which satisfies the condition

$$P_{\text{proposal}}(U_n \rightarrow U_p) = P_{\text{proposal}}(U_p \rightarrow U_n). \tag{4.5}$$

2. The acceptance probability is calculated as

$$P_{\text{acceptance}}(U_n \rightarrow U_p) = \min\left(1, e^{S[U_n]-S[U_p]}\right). \tag{4.6}$$

3. The next configuration U_{n+1} is chosen to be either the proposed configuration or current
   configuration, with probability $P_{\text{acceptance}}$ or $1 - P_{\text{acceptance}}$ respectively.

The exact form of the proposal distribution $P_{\text{proposal}}(U_n \rightarrow U_p)$ is not explicitly specified by the
method, but can be any distribution which satisfies the condition (4.5). Given that, then the
condition (4.4) is also satisfied, since for

$$P(U_{n+1} \rightarrow U_n) = P_{\text{proposal}}(U_n \rightarrow U_{n+1})P_{\text{acceptance}}(U_n \rightarrow U_{n+1}), \tag{4.7}$$

we have

$$\frac{P(U_n \to U_{n+1})}{P(U_{n+1} \to U_n)} = \frac{P_{\text{proposal}}(U_n \to U_{n+1})}{P_{\text{proposal}}(U_{n+1} \to U_n)} e^{S[U_n]-S[U_{n+1}]} = \frac{e^{-S[U_{n+1}]}}{e^{-S[U_n]}}. \tag{4.8}$$

There will clearly be some level of autocorrelation - the correlation between subsequent configurations U_n and U_{n+1} - and so to use this algorithm effectively, sufficiently many iterations should be completed before selecting the first configuration for the ensemble, and again sufficiently many iterations should be completed between each subsequent selected configuration for the ensemble. In each case, the number of iterations that this should be depends on the autocorrelation, which will vary depending on the system that is being simulated.

4.2.1   Estimating Errors

Due to the correlation between elements in the selected sample of configurations, and measurements of observables performed on those configurations, the usual method for estimating the error in the measurements as their standard deviation divided by $\sqrt{N}$ will not be correct. Instead, a method known as bootstrapping allows the errors to be estimated correctly even when the configurations in the sample are not independent [21].

The procedure for this consists of randomly resampling from the selected ensemble of configurations: A random sample of N configurations is selected from the ensemble (allowing the same configuration to be chosen more than once, so as not to simply end up with the original ensemble) and the expectation value of the observable is calculated for this new sample. This process of resampling is then repeated many times, and the standard deviation of the measurement for each of these gives an estimate of the error in the original measurement. Explicitly, if we have N configurations in the selected ensemble K then a measurement of the expectation value of an observable $\mathcal{O}$ is calculated as

$$\langle \mathcal{O} \rangle = \frac{1}{N} \sum_{U \in K} \mathcal{O}[U]. \tag{4.9}$$

Then we take R samples, K_r, of randomly chosen combinations, with repetition, of configurations $U \in K$, and calculate the expectation value of $\mathcal{O}$ for this sample

$$\langle \mathcal{O} \rangle_r = \frac{1}{N} \sum_{U \in K_r} \mathcal{O}[U] \tag{4.10}$$

(note that this sum includes the same term multiple times for configurations that have been selected more than once). We then calculate the error in $\langle\mathcal{O}\rangle$, $\sigma_{\mathcal{O}}$, as the standard deviation of $\langle\mathcal{O}\rangle_r$,

$$\sigma_{\mathcal{O}} = \sqrt{\frac{1}{R}\sum_{r=1}^{R}\left(\langle\mathcal{O}\rangle_r - \mu_{\mathcal{O}}\right)^2}, \tag{4.11}$$

where $\mu_{\mathcal{O}}$ is the mean of $\langle\mathcal{O}\rangle_r$, or simply $\langle\mathcal{O}\rangle$ as this is the value towards which the mean will tend for large R.

4.2.2   Reweighting of Samples

The Metropolis algorithm provides an efficient way to calculate quantities for a given action, but it is often desirable to calculate these quantities for a range of values for the non-dynamical parameters in the action, such as β and λ in the action (3.69). Alternative algorithms to the Metropolis algorithm are available to do this in an efficient way, such as the multicanonical method [22] which picks configurations according to the inverse density of states rather than their weights. This allows the same ensemble of configurations to be used in calculating quantities with different values of the parameters in the action, but also requires knowing, or computing, the density of states. However, the results of a Metropolis Monte Carlo run for an action with some fixed parameters can actually be used to provide estimates for the action with different values of those parameters [23]. This is known as reweighting and yields reasonable estimates provided that the configurations which contribute most to the partition function with the original set of parameters is not drastically different to the set of configurations that contribute most with the new parameters. This is due to the efficiency of the algorithm coming from its ability to quickly select those configurations that contribute the most and makes the method most useful when only making relatively small changes to the parameters, for example when searching for the exact critical value for a parameter at a phase transition.

To see how the method works, we will assume we are working with the action (3.69), but the idea generalises to any number of non-dynamical parameters in the action. To simplify notation we will

also define

$$P = \sum_{\mu<\nu} \sum_x \theta_{\mu\nu,x} \tag{4.12}$$

$$M = \sum_{\mu} \sum_x M_{\mu,x}, \tag{4.13}$$

so that the action for a specific choice of β and λ becomes $S_{\beta,\lambda}(P,M) = \beta P + \lambda M$. In the original run, configurations were selected from the probability distribution

$$P_{\beta,\lambda}(P,M) = \frac{1}{Z_{\beta,\lambda}} e^{-S_{\beta,\lambda}(P,M)} = \frac{1}{Z_{\beta,\lambda}} e^{-\beta P - \lambda M}, \tag{4.14}$$

where $Z_{\beta,\lambda} = \sum_{P,M} P_{\beta,\lambda}(P,M)$ ensures that the distribution is normalised. The probability distribution for different values of β' and λ', $P_{\beta',\lambda'}(P,M)$, can then be written in terms of $P_{\beta,\lambda}(P,M)$ as

$$\begin{aligned} P_{\beta',\lambda'}(P,M) &= \frac{1}{Z_{\beta',\lambda'}} e^{-S_{\beta',\lambda'}(P,M)} \\ &= \frac{1}{Z_{\beta',\lambda'}} e^{-\beta' P - \lambda' M} \\ &= \frac{Z_{\beta,\lambda}}{Z_{\beta',\lambda'}} P_{\beta,\lambda}(P,M) e^{(\beta-\beta')P + (\lambda-\lambda')M}. \end{aligned} \tag{4.15}$$

By requiring that the distribution is normalised, we can see that

$$\frac{Z_{\beta,\lambda}}{Z_{\beta',\lambda'}} = \sum_{P,M} P_{\beta,\lambda}(P,M) e^{(\beta-\beta')P + (\lambda-\lambda')M}. \tag{4.16}$$

The expectation value of an observable, for given β and λ is given by

$$\langle \mathcal{O} \rangle_{\beta,\lambda} = \sum_{P,M} \mathcal{O}(P,M) P_{\beta,\lambda}(P,M) \tag{4.17}$$

and in our original run the N configurations in the ensemble, having values P_n and M_n, have been selected according to $P_{\beta,\lambda}(P,M)$, so that the observable is estimated by taking the mean

$$\langle \mathcal{O} \rangle_{\beta,\lambda} = \frac{1}{N} \sum_{n=1}^{N} \mathcal{O}(P_n, M_n). \tag{4.18}$$

Using Equation (4.15) we can therefore estimate the observable for the action with parameters β' and λ' with the reweighted mean

$$\langle \mathcal{O} \rangle_{\beta',\lambda'} = \frac{1}{Z} \sum_{n=1}^{N} \mathcal{O}(P_n, M_n) e^{(\beta-\beta')P + (\lambda-\lambda')M}, \tag{4.19}$$

where here $Z = \sum_{n=1}^{N} e^{(\beta-\beta')P_n + (\lambda-\lambda')M_n}$ is the normalisation factor (4.16).

The general form of this, for an action $S_{\beta_r}[U]$ for configurations U and set of non-dynamical parameters β_r used in the action for the original run, is given by

$$\langle \mathcal{O} \rangle_{\beta'_r} = \frac{1}{Z} \sum_{n=1}^{N} \mathcal{O}[U_n] e^{S_{\beta_r}[U_n] - S_{\beta'_r}[U_n]} \tag{4.20}$$

$$Z = \sum_{n=1}^{N} e^{S_{\beta_r}[U_n] - S_{\beta'_r}[U_n]}. \tag{4.21}$$

To combine several Monte-Carlo runs at different values of the non-dynamical parameters, each run can be used to produce an estimate for the new parameter values, and these can be combined as a weighted mean, with the weight given by $\dfrac{1}{\sigma_i^2}$, where σ_i is an estimate of the error on the result from run i. A more optimised but slightly more complex procedure for combining multiple runs at different parameter values is given in [24].

4.3   Simulating the Compact U(1) Lattice Gauge Theory

4.3.1   Metropolis Procedure for Compact U(1)

The Metropolis algorithm described above can be applied to the compact U(1) lattice gauge theory of Section 3.5 by updating each link $\theta_{\mu,x}$ at for each μ and x individually, with the proposed new value for the parameter chosen at random from the uniform distribution on $[-\pi, \pi]$. Alternatively, $\theta_{\mu,x}$ can be updated by shifting its value by an amount chosen from the uniform distribution on $[-a, a]$, where $a < \pi$ is adjusted to optimise the process - smaller values of a generally result in a higher acceptance probability, but result in an increased autocorrelation between iterations. In each "sweep" of the lattice, every link is updated in a separate Metropolis step, and this is completed in a "checkerboard" fashion, as shown for two dimensions in Figure 3, first updating all the even links and then all the odd links.
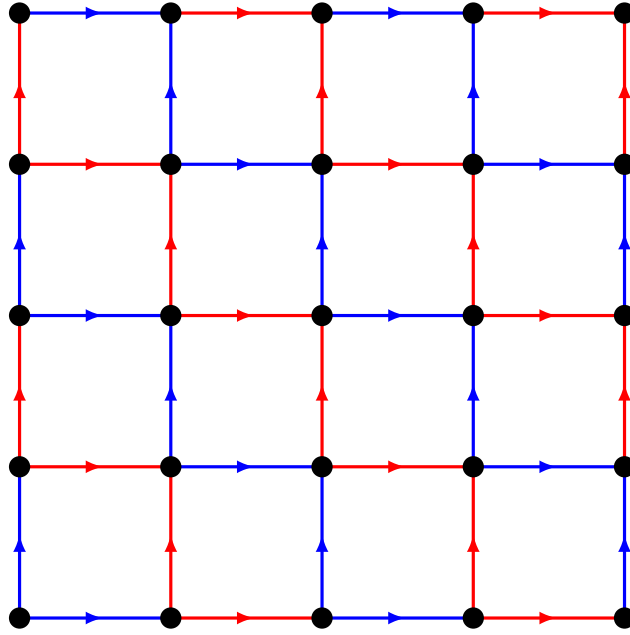
Figure 3: Even (blue) and odd (red) links are updated alternately.

When updating each link variable $\theta_{\mu,x}$, the probability of acceptance involves the value of the action for the old and new values of $\theta_{\mu,x}$, but rather than recalculating the entire action at each step, it is enough to simply calculate the change to the action due to the link being updated. For the action (3.47), with the link in the $\hat{\mu}$ direction, we first have the contribution from the six plaquettes surrounding the link - two plaquettes for each of the three axes orthogonal to $\hat{\mu}$ (one plaquette in each of the positive and negative directions along the axis). Secondly there are twelve cubes surrounding the link corresponding to the contributions to the monopole term - four cubes for each pair of the three axes orthogonal to $\hat{\mu}$ (one cube for each combination of positive and negative directions along these axes). These are shown in Figure 4 for a 3-dimensional lattice, where there are four plaquettes (one for each of the two axes orthogonal to $\hat{\mu}$) and four cubes (since there is only one pair of axes orthogonal to $\hat{\mu}$).

4.3.2   Boundary Conditions

In order to perform calculations using a finite lattice of length L on each side, suitable boundary conditions need to be imposed. The simplest choice, which preserves the spacetime symmetries of an infinite lattice, is periodic boundary conditions. This effectively embeds the lattice on a 4-torus,
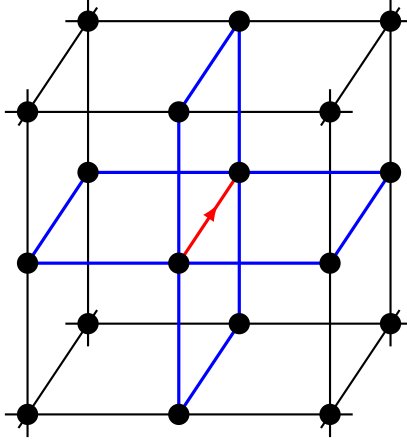
Figure 4: Four cubes, with four plaquettes (blue), surrounding the updated link (red).

and are defined by the effect on the link variables

$$\theta_{\mu,x+L\hat{\nu}} = \theta_{\mu,x}. \tag{4.22}$$

However, with these boundary conditions, the total monopole flux through the 3-d hypersurface in the lattice taken by summing over three of the four dimensions, and hence also the total magnetic charge in the lattice, will equal zero

$$\sum_{x_\mu, x_\nu, x_\sigma} M_{\rho,x} = 0. \tag{4.23}$$

This is clear to see from the definition of M_ρ, given in Equation (3.67), as when summing over the three dimensions orthogonal to the monopole flux each plaquette included in the first term will be cancelled from the same plaquette being included in the second term.

An alternative set of boundary conditions, which do allow non-zero total flux, are antiperiodic boundary conditions

$$\theta_{\mu,x+L\hat{k}} = -\theta_{\mu,x}. \tag{4.24}$$

where $\hat{k}$ is a spatial direction, and we retain periodic boundary conditions in the time direction. These boundary conditions are equivalent to charge conjugation and so are also known as C-periodic boundary conditions. This also means that while they appear to break translation invariance, the charge conjugation symmetry of the theory prevents this from being the case. The total flux given in Equation (4.23) can now be non-zero since the terms at the boundary no longer cancel due to the changed sign in the first term when the boundary is crossed. However, when summing over all

dimensions it is again found that they cancel. To avoid this we can introduce twisted boundary conditions.

Like C-periodic boundary conditions, twisted boundary conditions do not break any symmetries of the theory as they are equivalent to a gauge transformation. The idea is that a gauge transformation is applied at the spatial boundaries which modifies the monopole flux which does not cancel so that there is an overall magnetic charge in the lattice. Again periodic boundary conditions are still used for the time direction. By redefining the variables via the appropriate gauge transformation, the introduced flux can be spread homogeneously across the lattice so that it does not break translation invariance. This technique has been used in a number of studies of monopoles in lattice gauge theories, for example for SU(2) in [25]. For compact U(1) the technique was used in [26], where the twist was applied to a "stack" of plaquettes in one spatial dimension, and the twist could be chosen to introduce an arbitrary flux, $\theta_3 \to \theta_3 + \phi$. The twist was also applied in combination with antiperiodic boundaries, applied to one stack in each of the three spatial dimensions, preserving rotational symmetry, and with the flux introduced by the twist required to be equal to π, so that the quantisation of the monopole flux is preserved. This is implemented by using the boundary conditions on the links

$$
\begin{aligned}
\theta_1(t, 0, y + N, z) &= \pi - \theta_1(t, 0, y, z) \\
\theta_2(t, x, 0, z + N) &= \pi - \theta_2(t, x, 0, z) \\
\theta_3(t, x + N, y, 0) &= \pi - \theta_3(t, x, y, 0),
\end{aligned}
\tag{4.25}
$$

with antiperiodic boundary conditions for the remaining points on the spatial boundaries, and periodic boundary conditions at the time boundary. For these boundary conditions to be consistent, the flux applied at the twist must be a multiple of π. Figure 5 shows the links and plaquettes where the twist is applied. With the twisted boundary conditions there will now be an overall magnetic charge in the system and so the properties of the monopole can be more easily investigated, as we will see in Chapter 5.

4.3.3   Critical Slowing Down and the Dynamical Parameter Method

One issue that can occur with the Metropolis algorithm with these local updates is that if there are multiple local minima in the action then it is possible for the algorithm to get stuck around that
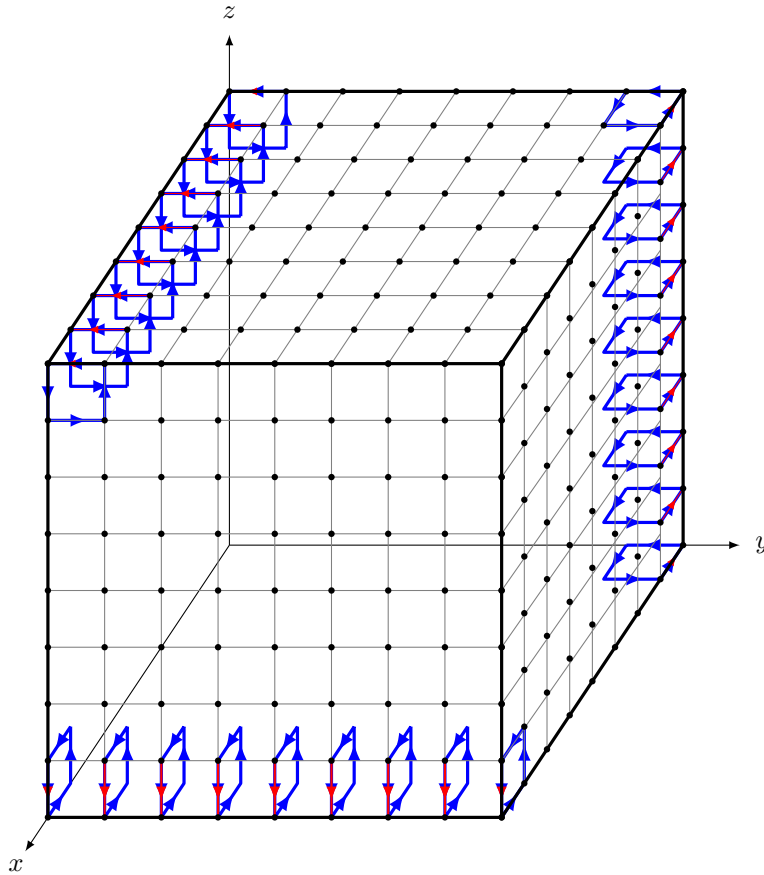
Figure 5: Plaquettes (blue) and links (red) where the twisted boundary conditions are applied.

minimum, taking some time to "tunnel" out into another minimum; this is known as critical slowing down. One way to solve the problem of critical slowing down is to use a non-local update, such as in the multi-grid method [27] where, in addition to local updates of the individual variables, updates on multiple points are proposed simultaneously. Another alternative is to use the multicanonical method mentioned in Section 4.2.2 since this picks configurations in a way unaffected by the energy profile. For our purposes however, the Metropolis algorithm with local updates will suffice, except for one modification used to avoid critical slowing down in the specific theory that we are studying.

The dynamical parameter method [28] for solving this problem was introduced to avoid critical slowing down close to the phase transition in the compact U(1) lattice gauge theory with monopole term. Around the phase transition the two phases coexist but with an energy barrier preventing the Metropolis algorithm from tunnelling between them, particularly for negative λ where the strength of the first order transition is stronger. For larger (positive) values of λ the transition eventually becomes of second order and the issue of tunnelling through an energy barrier is removed. This

can be taken advantage of in calculations by allowing λ to become a dynamical parameter of the Metropolis algorithm. For the negative values of λ an easier route becomes available for tunnelling from configurations in one phase to those in another by going via the values of λ where there is no large energy barrier preventing the transition.

With λ fixed, we have the probability distribution

$$P_\lambda(U) = \frac{1}{Z_\lambda} e^{-S_\lambda(U)} \tag{4.26}$$

and with λ a dynamical parameter, we require that the probability at any given value of λ takes the same form. This means that the joint probability distribution for λ and U must take the form

$$P(U, \lambda) = f(\lambda) P_\lambda(U), \tag{4.27}$$

where $f(\lambda)$ will be made approximately constant to ensure that each value of λ is equally likely. We then define the new joint action $S(U, \lambda)$

$$S(U, \lambda) = S_\lambda(U) + g(\lambda), \tag{4.28}$$

where

$$g(\lambda) = -log\left(f(\lambda)\frac{Z}{Z_\lambda}\right), \tag{4.29}$$

so that the joint probability distribution has the form

$$P(U, \lambda) = \frac{1}{Z} e^{-S(U, \lambda)}. \tag{4.30}$$

Then, after updating each of the link variables in the Metropolis algorithm in the usual way, one additional Metropolis step is completed to update the value of λ, which can take one of n fixed values, λ_q, ordered such that $\lambda_{q+1} > \lambda_q$. The proposed value $\lambda_{q'}$ is chosen using the proposal matrix $\frac{1}{2}(\delta_{q+1,q'} + \delta_{q,q'+1} + \delta_{q,1}\delta_{q',1} + \delta_{q,n}\delta_{q',n})$, which is then accepted according to the probability $\min(1, e^{S(U,\lambda_q)-S(U,\lambda_{q'})})$ so that the probability of transitioning from λ_q to $\lambda_{q'}$ is given by

$$P(U, q \to q') = \frac{1}{2}\min(1, e^{S(U,\lambda_q)-S(U,\lambda_{q'})}). \tag{4.31}$$

For each value of λ, values of $\beta(\lambda)$ and $g(\lambda)$ are required. For the largest value of λ, λ_1, the value of $g(\lambda_1)$ can be chosen arbitrarily, since it is only the differences $g(\lambda_{q+1}) - g(\lambda_q)$ that matter, and $\beta(\lambda_1)$ should be chosen such that the two phases coexist and the tunnelling time between them is reasonably short. This can be done using short Metropolis runs at fixed λ and β. The values of $g(\lambda_q)$ are determined by the requirement for $f(\lambda_q) \approx$ const.; this implies that $g(\lambda_q) \approx \ln Z_{\lambda_q} +$const. which can be estimated from short runs at fixed λ followed by iteratively improving the values by making the replacement $g(\lambda_q) \rightarrow g(\lambda_q) + \ln(f(\lambda_q))$. Alternatively, when searching for the critical value, $\beta_c(\lambda)$, of the phase transition the values for both $\beta(\lambda_q)$ and $g(\lambda_q)$ can be efficiently determined simultaneously using an iterative process, allowing longer runs using the dynamical parameter method to then be completed for the precise value of $\beta_c(\lambda)$ to be determined using the reweighting procedure described in Section 4.2.2. Starting from λ_1, with $\beta(\lambda_1)$ already determined and $g(\lambda_1)$ arbitrarily set to 0, the values of $\beta\lambda_q$ and $g(\lambda_q)$ are determined in sequence from $\beta\lambda_{q-1}$ and $g(\lambda_{q-1})$. Equation (4.31) and detailed balance imply that

$$f(\lambda_{q-1})P_{q-1}(U)P(U, q-1 \rightarrow q) = f(\lambda_q)P_q(U)P(U, q \rightarrow q-1). \tag{4.32}$$

If we then consider subsets $K(q)$ of configurations U with the weight

$$w_K(q) = \sum_{U \in K(q)} P_{\lambda_q}(U), \tag{4.33}$$

then the average transition probability for the set is given by

$$p_K(q \rightarrow q') = \sum_{U \in K(q)} P_{\lambda_q}(U)P(U, q \rightarrow q'). \tag{4.34}$$

Equation (4.32) then implies that, for the set $K(q)$,

$$f(\lambda_{q-1})w_K(q-1)p_K(q-1 \rightarrow q) = f(\lambda_q)w_K(q)p_K(q \rightarrow q-1). \tag{4.35}$$

The two subsets that we are interested in are the set of configurations in the "hot" condensate phase, K_c and the set of configurations in the "cold" Coulomb phase, K_h. These sets can be considered to be approximately independent, with vanishing probability of transitions between them, precisely due to the critical slowing down that is the reason for this dynamical parameter method. This also means that relatively short Monte–Carlo runs starting from a "cold" state with the all link parameters initially set to zero, and a "hot" state with all link parameters set to random

values, will select only configurations from K_c and K_h respectively. To get close to the critical value $\beta_c(\lambda_q)$, the condition that the two phases are equally probable is imposed, which implies that the weights are equally probable, $w_{K_c} = w_{K_h}$. Assuming that the two subsets cover the whole set of configurations (configurations that have a very low probability can be safely ignored), the weights will then be given by

$$w_{K_c}(q) = w_{K_h}(q) = \frac{1}{2}. \tag{4.36}$$

Using this condition, $f(\lambda) \approx$ const., and Equation (4.35) applied to each set, we find that

$$\begin{aligned} p_{K_c}(q - 1 \to q) &= p_{K_c}(q \to q - 1) \\ p_{K_h}(q - 1 \to q) &= p_{K_h}(q \to q - 1). \end{aligned} \tag{4.37}$$

An initial estimate of $\beta(\lambda_q)$ can be produced either by extrapolating from values for lower λ or by reweighting the MC run at λ_{q-1} and searching for the value of which satisfies the condition (4.36). Then, after a short Monte-Carlo run with this estimate at fixed λ_q, from hot and cold starts to produce sets of configurations in each phase, the average transition probabilities (4.34) can be estimated as

$$p_{K_i}(q \to q') \approx \frac{1}{N_{K_i(q)}} \sum_{U \in K_i(q)} P(U, q \to q'), \tag{4.38}$$

where $N_{K_i}(q)$ is the number of configurations in the set produced by the Monte-Carlo run. Since this approximation depends on $P(q \to q')$, which depends on $\beta(\lambda_q)$ and $g(\lambda_q)$, their values can be adjusted until the conditions (4.37) are satisfied. This process can be repeated for subsequent values of λ_q to obtain estimates for all $\beta(\lambda_q)$ and $g(\lambda_q)$. The dynamical parameter method can then be used with these values and, if required, improved values of $\beta(\lambda_q)$ and $g(\lambda_q)$ obtained by the same procedure. This procedure from [28], can actually be slightly improved by reweighting the sets used in the approximation (4.38) when adjusting the value of $\beta(\lambda_q)$, using the reweighting procedure outlined in Section 4.2.2.

5 Monopole Properties in Compact U(1) on the Lattice

5.1 Finding the Critical Point for the Phase Transition

The first step in investigating the properties of monopoles in the compact U(1) lattice gauge theory is to determine the regions where the theory is confining. In our case this amounts to finding the critical value, β_c, of β for a given λ, for the phase transition between the confinement phase of a monopole condensate and deconfined Coulomb-like phase. This was achieved using the method outlined in Section 4.3.3, for a lattice size 8^4, with periodic boundary conditions. Table 1 shows the results, and Figure 6 shows histograms of the average plaquette energy

$$E = \frac{1}{6L^4} \sum_x \sum_{\mu < \nu} (1 - \cos \theta_{\mu\nu,x}). \tag{5.1}$$

These are both in agreement with [29] for the range $\lambda = -0.3 - 0$, with Figure 6 clearly showing the splitting of the peaks indicating the strengthening of the first order phase transition. For more negative values of λ this splitting of the two phases is seen to continue until around $\lambda \sim -1.6$ where there is evidence of a tricritical point, with a third phase consisting of monopoles throughout the lattice at almost every lattice site. This new phase and its transition was not investigated further since for $\beta > \beta_c$ the Coulomb phase in which we are most interested continues to exist at all values of λ that were investigated, while for $\beta > \beta_c$ either the usual confinement phase or the new phase is found. Figure 7 shows the three peaks appearing in the distributions of the average plaquette energy (5.1) and monopole density

$$\rho = \frac{1}{4L^4} \sum_x \sum_\mu |M_{\mu,x}|, \tag{5.2}$$

indicating the three phases at the tricritical point.

The position of the phase transition was also found not to significantly differ when using C-periodic or twisted boundary conditions in place of periodic boundary conditions. The above values for the critical value of β for a given λ can therefore be used to choose an appropriate range of λ and β when investigating the monopole properties.

λ	β_c	$g(\lambda) - g(0)$
0.0	1.007	0.00
-0.1	1.065	-401.71
-0.2	1.122	-780.05
-0.3	1.179	-1134.91
-0.4	1.236	-1475.51
-0.5	1.294	-1799.63
-0.6	1.352	-2110.64
-0.7	1.411	-2410.39
-0.8	1.470	-2700.35
-0.9	1.531	-2981.90
-1.0	1.592	-3255.56
-1.2	1.718	-3782.52
-1.4	1.849	-4287.37

Table 1: Critical value β_c for the phase transition and value of $g(\lambda)$ used for the simulations at λ on an $L = 8$ lattice.
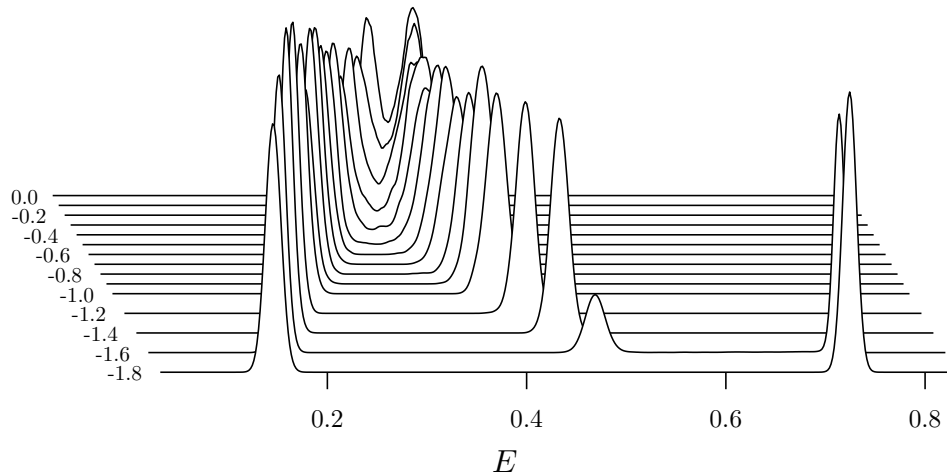

Figure 6: Distributions of the plaquette energy E for values of λ from -1.8 to 0 on a lattice of size $L = 8$.

5.2 The Monopole Mass

The mass of the monopole is an important property to measure; in the compact U(1) theory with no monopole term the mass is generally large and increases with the lattice size. In order to investigate the properties of monopoles that could correspond to the type of monopole potentially observable in experiments, it is necessary to reduce study a theory on the lattice where the mass is reduced. It is hoped that the addition of the monopole term with a negative value of λ will achieve this. A number of techniques have been used by other groups for measuring the mass of the monopole in compact U(1) lattice theory. The mass has been measured using monopole correlation functions formed from a monopole-antimonopole creation operator [30] and in the dual $\mathbb{Z}$ lattice gauge theory of compact U(1) [31]. In our case, two methods of measuring the mass have
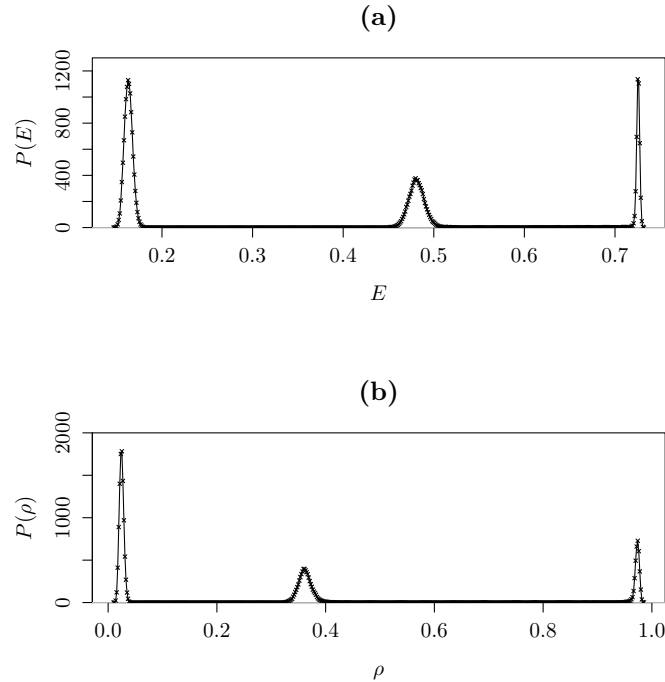
Figure 7: Distributions near the tricritical point $\lambda = -1.6$, $\beta = 1.99$ for lattice with $L = 8$, (a) for the average plaquette energy E and (b) for the average monopole density ρ.

been used both of which have been successfully used in other systems, for example in measuring the mass of the 't Hooft-Polyakov monopole in the lattice theory of the Georgi-Glashow SU(2) model [32].

5.2.1   Measuring the Mass Using the Free Energy

The twisted and C-periodic boundary described in Section 4.3.2 fix the total magnetic charge in the system to odd or even respectively. In the Coulomb phase the monopoles are expected, for a large enough lattice, not to interact. This allows us to determine the monopole mass, M. The partition function (3.49) for the system with n net units of magnetic charge, Z_n is related to that with no net magnetic charge, Z_0, in the Coulomb phase by [32]

$$Z_n = Z_0 e^{-|n|MT}, \tag{5.3}$$

where T is the length of the time dimension of the lattice. The mass is then given by

$$M = -\frac{1}{T}\ln\frac{Z_1}{Z_0} = \frac{1}{T}(F_1 - F_0),\tag{5.4}$$

where F_1 and F_0 are the free energies for the systems with one net unit of magnetic charge and no net magnetic charge respectively, using the definition of the free energy $F = -\ln Z$. The C-periodic boundary conditions have an even overall magnetic flux and so with higher values of n suppressed, the partition function will take the form $Z_{\text{CP}} = Z_0$. Likewise for twisted boundary conditions, with an odd net charge, the partition function will take the form $Z_{\text{T}} = 2Z_1 = 2Z_0 e^{-MT}$, and so these two partition functions, or the two corresponding free energies, could be used to find the monopole mass. Using Monte-Carlo calculations, however, the free energy is not a quantity that can be measured. We need to find a quantity in the form of a measurable observable (3.50). The derivative of the free energy with respect to some parameter x of the action has exactly this form, since

$$\begin{aligned}
\frac{\partial F}{\partial x} &= \frac{\partial}{\partial x}\left(-\ln Z\right)\\
&= -\frac{1}{Z}\frac{\partial}{\partial x}Z\\
&= -\frac{1}{Z}\frac{\partial}{\partial x}\int dU\, e^{-S[U]}\\
&= \frac{1}{Z}\int dU\,\frac{\partial S}{\partial x}e^{-S[U]}\\
&= \left\langle\frac{\partial S}{\partial x}\right\rangle.
\end{aligned}\tag{5.5}$$

The derivative of the mass with respect to x can therefore be measured as

$$\frac{\partial M}{\partial x} = \frac{1}{T}\left(\left\langle\frac{\partial S}{\partial x}\right\rangle_{\text{T}} - \left\langle\frac{\partial S}{\partial x}\right\rangle_{\text{CP}}\right),\tag{5.6}$$

where $\langle\,\cdot\,\rangle_{\text{T}}$ and $\langle\,\cdot\,\rangle_{\text{CP}}$ refer to the expectation values measured in lattices with twisted and C-periodic boundary conditions respectively. If we take x to be λ of the action (3.69), this tells us how the mass scales with λ.

$$\frac{\partial M}{\partial\lambda} = \frac{1}{T}\left(\left\langle\frac{\partial S}{\partial\lambda}\right\rangle_{\text{T}} - \left\langle\frac{\partial S}{\partial\lambda}\right\rangle_{\text{CP}}\right).\tag{5.7}$$

Then, if the mass is known at some value λ_0 of λ, we can perform an integration from that point to determine the value of the mass at another value, λ_1,

$$M(\lambda_1) = M(\lambda_0) + \int_{\lambda_0}^{\lambda_1} d\lambda \, \frac{1}{T} \left(\left\langle \frac{\partial S}{\partial \lambda} \right\rangle_{\text{T}} - \left\langle \frac{\partial S}{\partial \lambda} \right\rangle_{\text{CP}} \right). \tag{5.8}$$

5.2.2   Measuring the Mass Using Correlation Functions

The second method for measuring the mass is using correlation functions. This has the advantage that it does not require performing the numerical integration needed when using the free energy difference, and so is less computationally intensive, requiring only computing results at the values of λ at which the mass is desired. For a two-point correlation function, if we insert a complete set of energy eigenstates $\sum_\alpha |\alpha\rangle \langle\alpha|$ satisfying $\hat{H} |\alpha\rangle = E_\alpha |\alpha\rangle$, and take the fourier transform, we obtain

$$\begin{aligned} C(\mathbf{k}, t) &= \langle 0| \mathcal{O}(\mathbf{k}, 0)\mathcal{O}(\mathbf{k}, t) |0\rangle \\ &= \sum_\alpha \sum_\mathbf{x} \sum_\mathbf{y} \langle 0| \mathcal{O}(\mathbf{x}, 0)e^{i\mathbf{k}\cdot\mathbf{x}} |\alpha\rangle \langle\alpha| e^{-i\mathbf{k}\cdot\mathbf{y}} \mathcal{O}(\mathbf{y}, t) |0\rangle \, e^{-E_\alpha t}. \end{aligned} \tag{5.9}$$

where the discrete Fourier transform corresponds to a sum over the lattice points, rather than the usual integral of continuous Fourier transforms (note also that this is the form after having performed the Wick rotation to imaginary time). Due to the exponential factor $e^{-E_\alpha t}$, this correlation function can be approximated by only taking the contribution from the lowest energy state.

The most obvious correlator to use would be the monopole correlator, where $\mathcal{O} = M_\mu$. In the Coulomb phase, assuming that the lowest energy state is non-relativistic, we would have

$$C(\mathbf{k}, t) \sim e^{-\frac{k^2}{2M}t}, \tag{5.10}$$

where $k = |\mathbf{k}|$ is the magnitude of the lowest possible momentum and M is the monopole mass. On the lattice, with periodic boundary conditions, the allowed momenta in a given direction are quantised as $k_i = \dfrac{2\pi n}{L}$, for $n \in \mathbb{Z}$, since the length of the lattice must be an integer number of wavelengths. For anti-periodic (or twisted) boundary conditions, if $\mathcal{O}$ is even under charge conjugation, the allowed momenta are $k_i = \dfrac{(2n-1)\pi}{L}$ since now there must be a half integer number of wavelengths along the length of the lattice; for even functions the allowed momenta are the same as for periodic boundary conditions. However, it is difficult to measure this correlator;

due to the discrete nature and small values of M_μ, long runs of the Monte-Carlo procedure would be required to reduce the errors to an acceptable level.

Alternatively we can use a plaquette correlator where $\mathcal{O} = \bar{\theta}_{\mu\nu}$, or $\mathcal{O} = \sin\theta_{\mu\nu}$, either of which has the continuum limit $C(\mathbf{k},t) = \langle 0 | F_{\mu\nu} F_{\rho\sigma} | 0 \rangle$. For periodic or anti-periodic boundary conditions, we have

$$C(\mathbf{k},t)_{\text{P,CP}} = \langle \sin\theta_{\mu\nu} \sin\theta_{\rho\sigma} \rangle_{\text{P,CP}} \sim e^{-kt}. \tag{5.11}$$

However with twisted boundary conditions introducing a monopole into system, the lowest energy contribution to the correlator is now expected to be from coupling to the monopole, in which case we again have

$$C(\mathbf{k},t)_{\text{T}} = \langle \sin\theta_{\mu\nu} \sin\theta_{\rho\sigma} \rangle_{\text{T}} \sim e^{-\frac{k^2}{2M}t}. \tag{5.12}$$

This suggests that measuring this correlation function on a lattice with twisted boundary conditions will allow us to determine the monopole mass.

5.2.3   Numerical Results for the Monopole Mass

Values for $\dfrac{dM}{d\lambda}$ were calculated using the difference in the derivative of the free energy for twisted and C-periodic boundary conditions (5.7), for values of λ ranging from -1 to 0 with $\beta = 1.6$, where the system is in the Coulomb phase, for lattices of size $L = 8$ and $L = 12$. 200,000 Metropolis sweeps were performed at $L = 8$ and 150,000 sweeps at $L = 12$. These results are shown in Figure 8. As can be seen, the mass does decrease as λ is decreased, as expected. As the system gets closer to the transition from the Coulomb phase to the confinement phase, where we expect the monopole mass to vanish, the derivative of the mass increases faster than exponentially. This would suggest that for a given value of β, it should indeed be possible to reduce the monopole mass as desired by including the monopole term in the action with a negative value of λ.

Calculations using the plaquette correlation function (5.12) were performed for the same Monte-Carlo runs as above, using the minimum momentum $\mathbf{k} = (k,k,k)$, $k = \dfrac{\pi}{L}$. In order to take into account the periodicity of the lattice in the time direction, the correlation functions are fitted to

$$C(\mathbf{k},t) + C(\mathbf{k},T-t) \sim \begin{cases} e^{-kt} + e^{-k(t-T)}, & \text{C-periodic boundaries} \\ e^{-\frac{k^2}{2M}t} + e^{-\frac{k^2}{2M}(t-T)}, & \text{twisted boundaries} \end{cases}. \tag{5.13}$$
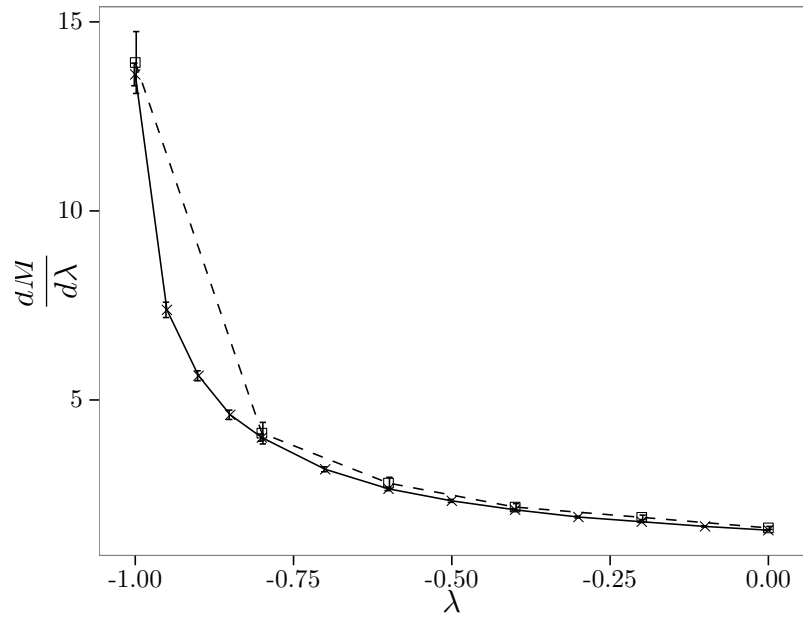
Figure 8: Values for $\frac{dM}{d\lambda}$ calculated using the difference between the derivative of the free energy with respect to λ for twisted and C-periodic boundary conditions. The solid line and squares represent the lattice size $L = 8$ while dashed line and crosses, represent $L = 12$.
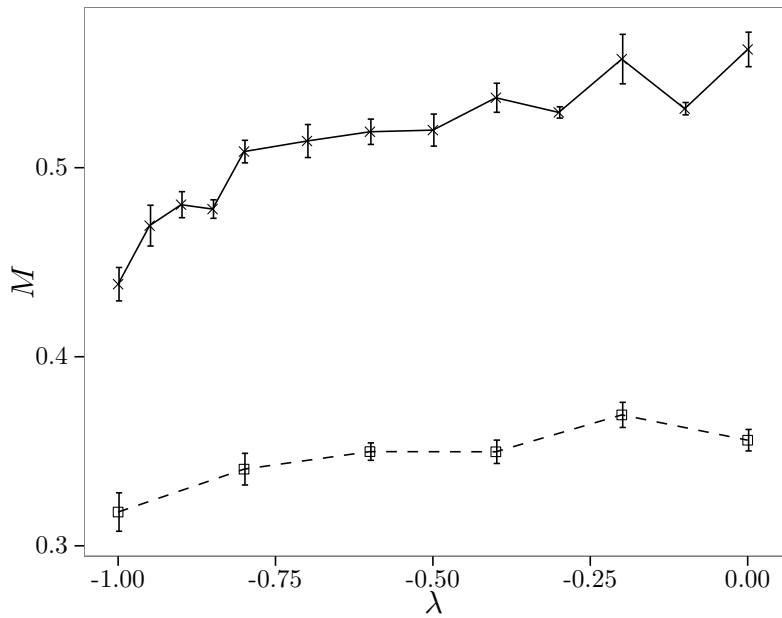

Figure 9: Preliminary results for M calculated using the plaquette correlation function for twisted boundary conditions. The solid line and squares represent the lattice size $L = 8$ while dashed line and crosses, represent $L = 12$.

With C-periodic boundary conditions, there was good agreement with the expected form, and the fitted value of k matched $k = \dfrac{\pi}{L}$ within the statistical errors. With twisted boundary conditions, the mass does scale in roughly the expected manner, however the overall normalisation appears to be incorrect. This is expected to be due to an error in the calculation algorithm and it is hoped that corrected results will agree with the results from using the free energy method. Figure 9 shows the preliminary results obtained so far.

6 Conclusion

As has been shown, magnetic monopoles, despite there being so far no experimental evidence for their existence, have a number of theoretical motivations that suggest that they do exist but have simply not yet been observed. For a start their existence would introduce an electric-magnetic duality, making the unification of the electric and magnetic forces more elegant and natural. In addition their introduction would require the electric (and magnetic) charge to be quantised - an effect that has been observed in all known particles. It even seems likely that any theory which truly explains the quantisation of the electric charge will contain monopoles. Most strikingly, however, is that all Grand Unified Theories - theories that attempt to combine electromagnetism with the weak and strong nuclear forces into a single unified quantum field theory - are guaranteed to predict the existence of monopoles, and this is also true for theories of everything which include gravity in addition to the other forces. We therefore have strong reasons to believe that studying these particles could lead to insights that improve our understanding of the laws of Nature.

As we have seen, the concept of a lattice gauge theory provides a framework with many advantages over other methods for investigating the quantum field theories that describe the world. The discretisation of spacetime provides a cut-off which regularises the theory, and using the tools available from statistical mechanics, efficient computations can be performed to calculate physical quantities. Unlike perturbative methods, lattice field theory can be used in the strong-coupling regime and for investigating states which are not simple perturbations of the vacuum state due their topology. This all makes lattice field theory a clear choice for investigating the properties of monopoles.

The compact U(1) lattice gauge theory - the lattice version of pure gauge quantum electrodynamics - contains magnetic monopoles of finite mass. As expected, in the continuum limit this mass tends towards infinity, however with the addition of a new term in the action which is proportional to the number of monopoles, with a negative coefficient, can counteract the diverging monopole mass as the continuum limit is taken. This could allow the properties of magnetic monopoles to be studied on a simple system that is still physically relevant. The results given here, although only preliminary in some respects, have demonstrated that the mass can indeed be controlled by the choice of the coefficient of this additional term.

There are many aspects of this investigation that could warrant further research. The use of the correlation functions in measuring the mass does not yet appear to fully agree with measurements using free energy differences. If the reason for this could be found then it would allow similar calculations to be used in investigating other properties of the monopoles such as whether they act as point particles and how they interact with other particles. So far the mass of the monopole has only been studied at one value of the coupling β, and on relatively small lattices and short Monte-Carlo runs. It would be valuable to investigate the effect of the additional term in the action on monopoles for a range of values of β, and using a range of lattice sizes with longer calculation run times would show if and how the effect changes as the continuum limit is approached, in addition to giving more precise results. Such investigations into monopoles in the compact U(1) lattice gauge theory could prove to be experimentally relevant in searches for physical monopoles, making them worthwhile endeavours beyond just theoretical interest.

References

[1] Paul A. M. Dirac. Quantised singularities in the electromagnetic field. *Proceedings of the Royal Society of London. Series A*, 133(821):60–72, 1931.

[2] Y. Aharonov and D. Bohm. Significance of electromagnetic potentials in the quantum theory. *Phys. Rev.*, 115:485–491, Aug 1959.

[3] Michael E. Peskin and Dan V. Schroeder. *An Introduction To Quantum Field Theory (Frontiers in Physics)*. Westview Press, 1995.

[4] Gerard't Hooft. Magnetic monopoles in unified gauge theories. *Nuclear Physics B*, 79(2):276 – 284, 1974.

[5] Alexander M. Polyakov. Particle Spectrum in the Quantum Field Theory. *JETP Lett.*, 20:194–195, 1974.

[6] K.A. Olive and Particle Data Group. Review of particle physics. *Chinese Physics C*, 38(9):090001, 2014.

[7] John P. Preskill. Cosmological production of superheavy magnetic monopoles. *Phys. Rev. Lett.*, 43:1365–1368, Nov 1979.

[8] Alan H. Guth. Inflationary universe: A possible solution to the horizon and flatness problems. *Phys. Rev. D*, 23:347–356, Jan 1981.

[9] Arttu Rajantie. Introduction to magnetic monopoles. *Contemporary Physics*, 53(3):195–211, 2012.

[10] Franz J. Wegner. Duality in generalized ising models and phase transitions without local order parameters. *Journal of Mathematical Physics*, 12(10):2259–2272, 1971.

[11] Kenneth G. Wilson. Confinement of quarks. *Phys. Rev. D*, 10:2445–2459, Oct 1974.

[12] Jan Smit. *Introduction to quantum fields on a lattice: A robust mate*. Cambridge Lecture Notes in Physics. Cambridge University Press, 2002.

[13] T. A. DeGrand and Doug Toussaint. Topological excitations and monte carlo simulation of abelian gauge theory. *Phys. Rev. D*, 22:2478–2489, Nov 1980.

[14] James S. Barber, Robert E. Shrock, and Robert Schrader. A study of d=4 u(1) lattice gauge theory with monopoles removed. *Physics Letters B*, 152(34):221 – 225, 1985.

[15] James S. Barber and Robert E. Shrock. Dynamical shifting of the critical point in 4d u(1) lattice gauge theory. *Nuclear Physics B*, 257(0):515 – 530, 1985.

[16] S. Mandelstam. Vortices and quark confinement in non-abelian gauge theories. *Physics Letters B*, 53(5):476 – 478, 1975.

[17] Gerard 't Hooft. Gauge fields with unified weak, electromagnetic, and strong interactions. In *EPS International Conference on High Energy Physics*, pages 1225–1249, Palermo, 1975.

[18] Georges Ripka. *Dual Superconductor Models of Color Confinement*. Lecture Notes in Physics. Springer, 2004.

[19] J. Frhlich and P.A. Marchetti. Soliton quantization in lattice field theories. *Communications in Mathematical Physics*, 112(2):343–383, 1987.

[20] Nicholas Metropolis, Arianna W. Rosenbluth, Marshall N. Rosenbluth, Augusta H. Teller, and Edward Teller. Equation of state calculations by fast computing machines. *The Journal of Chemical Physics*, 21(6):1087–1092, 1953.

[21] B. Efron. Bootstrap methods: Another look at the jackknife. *The Annals of Statistics*, 7(1):1–26, 01 1979.

[22] Bernd A. Berg and Thomas Neuhaus. Multicanonical ensemble: A new approach to simulate first-order phase transitions. *Phys. Rev. Lett.*, 68:9–12, Jan 1992.

[23] Alan M. Ferrenberg and Robert H. Swendsen. New monte carlo technique for studying phase transitions. *Phys. Rev. Lett.*, 61:2635–2638, Dec 1988.

[24] Alan M. Ferrenberg and Robert H. Swendsen. Optimized monte carlo data analysis. *Phys. Rev. Lett.*, 63:1195–1198, Sep 1989.

[25] Arttu Rajantie and David J. Weir. Nonperturbative study of the 't hooft-polyakov monopole

form factors. *Phys. Rev. D*, 85:025003, Jan 2012.

[26] Michele Vettorazzo and Philippe de Forcrand. Electromagnetic fluxes, monopoles, and the order of 4d compact u(1) phase transition. *Nuclear Physics B*, 686(12):85 – 118, 2004.

[27] Jonathan Goodman and Alan D. Sokal. Multigrid monte carlo method for lattice field theories. *Phys. Rev. Lett.*, 56:1015–1018, Mar 1986.

[28] Werner Kerler, Claudio Rebbi, and Andreas Weber. Phase transition and dynamical-parameter method in u (1) gauge theory. *Nuclear Physics B*, 450(12):452 – 460, 1995.

[29] Werner Kerler, Claudio Rebbi, and Andreas Weber. Phase structure and monopoles in u(1) gauge theory. *Phys. Rev. D*, 50:6984–6993, Dec 1994.

[30] L. Polley and U.-J. Wiese. Monopole condensate and monopole mass in u(1) lattice gauge theory. *Nuclear Physics B*, 356(3):629 – 654, 1991.

[31] J. Jersák, T. Neuhaus, and H. Pfeiffer. Scaling analysis of the magnetic monopole mass and condensate in the pure u(1) lattice gauge theory. *Phys. Rev. D*, 60:054502, Jul 1999.

[32] Arttu Rajantie. Mass of a quantum 't hooft-polyakov monopole. *Journal of High Energy Physics*, 2006(01):088, 2006.